



# Review of the use of transition-metal-oxide and conducting polymer-based fibres for high-performance supercapacitors

Muhammad Amirul Aizat Mohd Abdah<sup>a</sup>, Nur Hawa Nabilah Azman<sup>a</sup>,  
Shalini Kulandaivalu<sup>a</sup>, Yusran Sulaiman<sup>a,b,\*</sup>

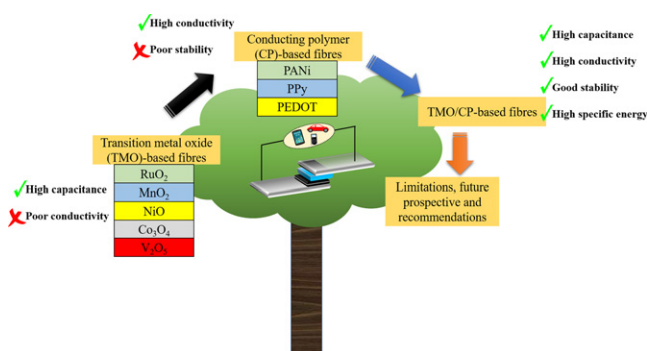
<sup>a</sup> Department of Chemistry, Faculty of Science, Universiti Putra Malaysia, 43400 UPM Serdang, Selangor, Malaysia

<sup>b</sup> Functional Devices Laboratory, Institute of Advanced Technology, Universiti Putra Malaysia, 43400 UPM Serdang, Selangor, Malaysia

## HIGHLIGHTS

- The classification and charge storage mechanism of supercapacitor are explained.
- Different types of nanofibres and their relationship with supercapacitor performance are discussed.
- Recent advances of transition-metal-oxide- and conducting polymer-based fibres are reviewed.
- The challenges and outlook of transition metal oxide/conducting polymer-based fibres in supercapacitors are highlighted.

## GRAPHICAL ABSTRACT



## ARTICLE INFO

### Article history:

Received 6 August 2019

Received in revised form 6 September 2019

Accepted 8 September 2019

Available online 13 September 2019

### Keywords:

Fibres  
Transition metal oxides  
Conducting polymers  
Supercapacitor

### Data availability:

The authors declare the data supporting the findings of this work is available within the article. Extra data is available from the authors upon request.

## ABSTRACT

There is a growing interest in the application of supercapacitors in energy storage systems due to their high specific power, fast charge/discharge rates and long cycle stability. Researchers have focused recently on developing nanomaterials to enhance their capacitive performance of supercapacitors. Particularly, the utilisation of fibres as templates has led to theoretical and practical advantages owing to their enlarged specific surface area, which allows fast electrolyte-ion diffusion. In addition, the inclusion of redox-active components, such as transition metal oxides (TMOs) and conducting polymers (CPs), into the fibres is believed to play an important role in improving the electrochemical behaviour of the fibre-based materials. Nevertheless, supercapacitors containing TMO- and CP-based fibres commonly suffer from inferior ion-transport kinetics and poor electronic conductivity, which can affect the rate capability and cycling stability of the electrodes. Therefore, the development of TMO/CP-based fibres has gained widespread attention because they synergistically combine the advantages of both materials, enabling revolutionary applications in the electrochemical field. This review describes and highlights recent progress in the development of TMO-, CP- and TMO/CP-based fibres regarding their design approach, configurations and electrochemical properties for supercapacitor applications, at the same time providing new opportunities for future energy storage technologies.

© 2019 The Authors. Published by Elsevier Ltd. This is an open access article under the CC BY-NC-ND license (<http://creativecommons.org/licenses/by-nc-nd/4.0/>).

\* Corresponding author at: Department of Chemistry, Faculty of Science, Universiti Putra Malaysia, 43400 UPM Serdang, Selangor, Malaysia.  
E-mail address: [yusran@upm.edu.my](mailto:yusran@upm.edu.my) (Y. Sulaiman).

## Contents

1. Introduction . . . . .	2
2. Supercapacitors and their mechanisms . . . . .	4
3. Strategies for NFs fabrication . . . . .	5
3.1. Electrospinning. . . . .	5
3.2. Carbon nanofibres . . . . .	5
4. Transition metal oxides . . . . .	7
4.1. Ruthenium-oxide-based fibres . . . . .	7
4.2. Manganese oxide-based fibres . . . . .	7
4.3. Nickel oxide-based fibres . . . . .	10
4.4. Cobalt oxide-based fibres . . . . .	10
4.5. Vanadium oxide-based fibres . . . . .	10
5. Conducting polymers . . . . .	11
5.1. Polyaniline-based fibres . . . . .	12
5.2. Polypyrrole-based fibres. . . . .	13
5.3. Poly(3,4 ethylenedioxythiophene)-based fibres . . . . .	14
6. Transition metal oxide/conducting polymer-based fibres . . . . .	15
7. Conclusions and outlook . . . . .	16
CRediT authorship contribution statement . . . . .	17
Acknowledgement . . . . .	17
References. . . . .	17

## 1. Introduction

In recent years, the development of sustainable and renewable energy storage systems has accelerated because of the need to preserve natural resources and control energy consumption. Non-conventional energy devices, such as batteries, supercapacitors and fuel cells, have been utilised in hybrid vehicles and portable electronic devices where the chemical energy is converted to electrical energy via electrochemical reactions [1]. Among them, supercapacitors or electrochemical capacitors (ECs) have attracted great attention due to their superior electrochemical performances, where high specific power, excellent cycling life and rapid charging/discharging rate [2] are highly desirable.

However, current supercapacitors still have low specific energy compared to batteries. To overcome this constraint, two main approaches have been extensively studied for enhancing the specific energy: (i) to fabricate advanced supercapacitors with high specific capacitance and (ii) to increase the voltage window from the selection of the electrolyte [3–6].

A good choice of electrode materials with remarkable electrical conductivity and a large specific surface area (SSA) is the main aspect for developing high-performance supercapacitors [7,8]. Fig. 1 shows the Ragone plot for different energy storage technologies: fuel cells, conventional batteries, supercapacitors and conventional capacitors. This graph explains the magnitude of specific energy (Wh/kg) and specific power

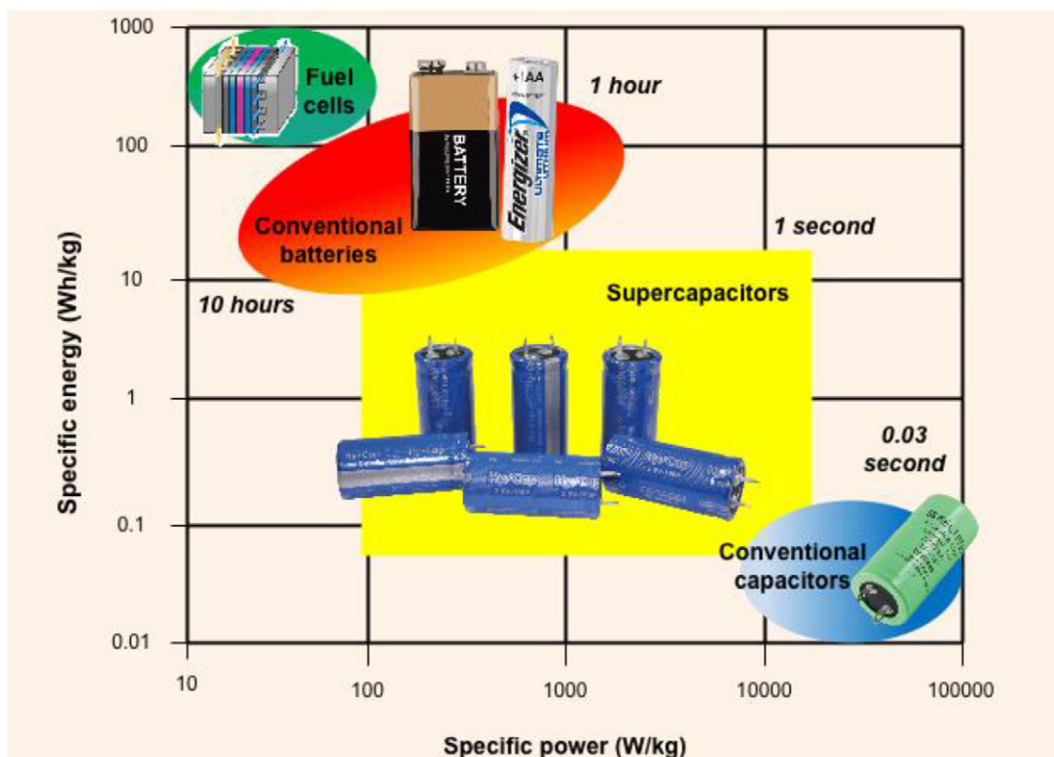


Fig. 1. Graph of specific energy versus specific power for different types of energy storage devices.

(W/kg) with discharging time for each device ( $E = Pt$ ). Although batteries can exhibit an excellent energy output (100–200 Wh/kg), they need additional time to be recharged, leading to a poor specific power performance [9]. Hence, supercapacitors are known as important members of the energy storage family due to their satisfying specific energy (1–10 Wh/kg), compared with traditional capacitors [10], and their higher specific power (500–10,000 W/kg) compared with batteries. Additionally, it is worth to mention that supercapacitors can be fully charged/discharged at a very fast rate with enlarged cycling lifetime [11]. In addition, the determination of the voltage windows entirely depends on the thermodynamic stability of the electrolytes. A maximum voltage window of 1.0 V was achieved using an aqueous electrolyte with a low equivalent series resistance (ESR). Although an organic electrolyte can be operated within a voltage window up to 3.0–5.0 V, it is hazardous to the environment and suffers from a high ESR, which inhibits achieving a high specific power [12]. Therefore, an aqueous electrolyte is commonly utilised in typical supercapacitors due to its low cost, availability and low toxicity [13].

Nanostructured materials and their composites are attractive hotspots for various applications such as drug delivery [14], biomedical (wound dressing) [15], tissue engineering [16], lithium-ion batteries (LIBs) [17] and supercapacitors [18–22]. One-dimensional (1D) nanomaterials, such as nanotubes, nanorods, nanobelts and nanofibres (NFs), possess unique features that can provide a high accessible surface area-to-

volume ratio and shorten the diffusion pathway for ion transportation [23,24]. Among all the kinds of nanomaterials, NFs are flexible for manufacturing various kinds of fibrous structures, such as hierarchical pores, core/shell structures, aligned and random fibres [25] (Fig. 2), which enhance the performance of energy storage devices. For example, Tran and Kalra [26] have prepared free-standing porous carbon nanofibres (CNFs) using a blend of polyacrylonitrile and sacrificial Nafion via electrospinning and subsequent carbonisation process. Nafion was used as pore-forming agent in the spinning solution, which thermally decomposed at high temperature. The porous CNFs showed a high specific surface area (1600 m<sup>2</sup>/g), yielding enhanced specific capacitance of 210 F/g. However, the poor specific energy (4 Wh/kg) limits their practical application for supercapacitor. The similar technique was employed by Xu [27] to synthesise NiCo<sub>2</sub>O<sub>4</sub>-CNFs@Ni(OH)<sub>2</sub> core-shell nanofibres. The uniform distribution of NiCo<sub>2</sub>O<sub>4</sub> nanoparticles on CNFs improves the contact between Ni(OH)<sub>2</sub> and NiCo<sub>2</sub>O<sub>4</sub>-CNFs which allows continuous transfer channels and short diffusion distances for electrolyte ions. The electrode possessed a specific capacitance as high as 1925 F/g with good stability of 87% after 5000 cycles. In addition, an oriented graphite fibres prepared by Yan et al. [28] exhibited the specific capacitance of 54.4 F/g which is less than the coal-derived carbon nanofibres (CCNFs) prepared by [29] with specific capacitance of 299.4 F/g. The significant improvement on the specific capacitance is due to the enlarged specific surface area from non-woven fibres of CCNFs which increase the accessible active

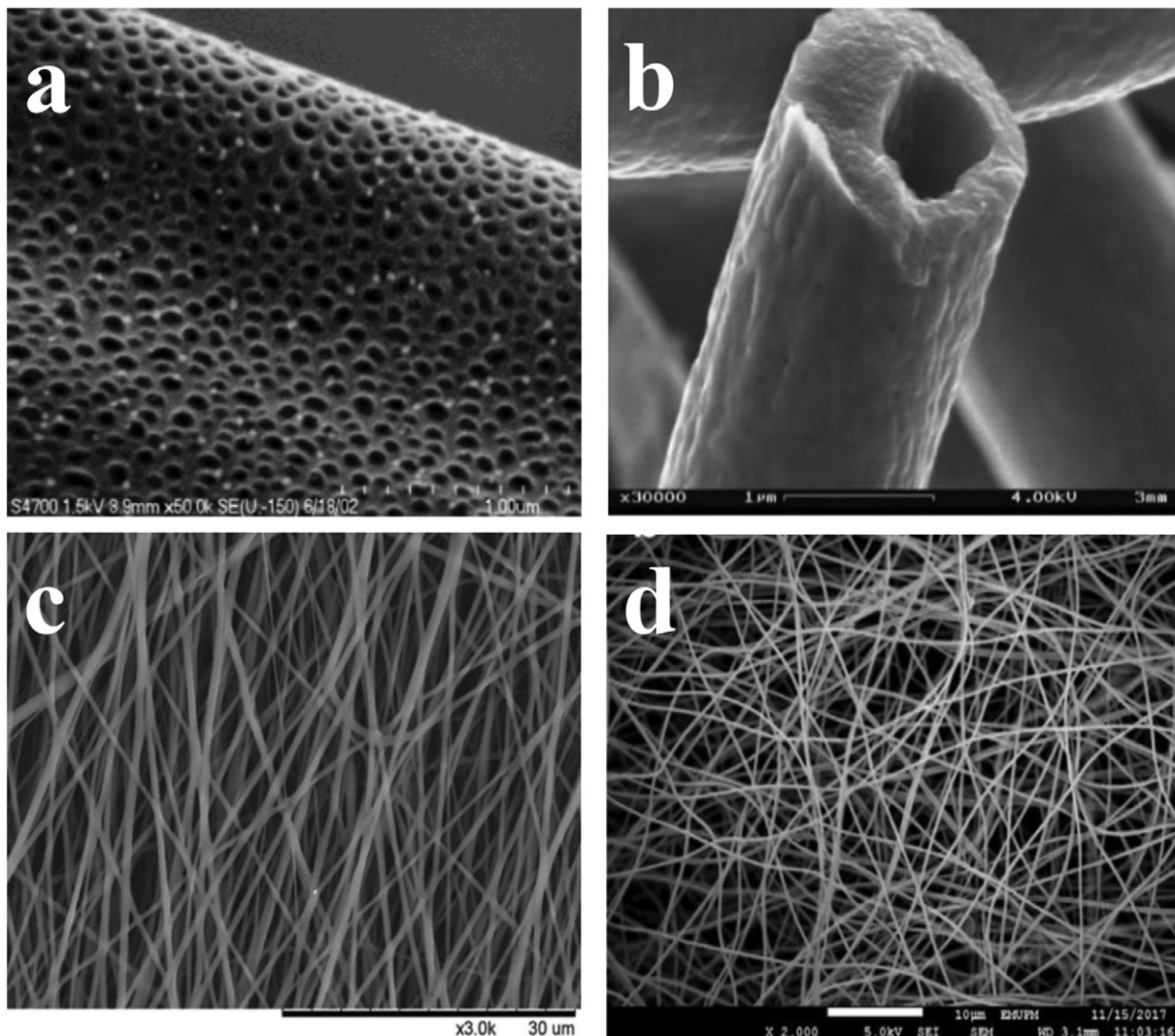


Fig. 2. Different morphologies of electrospun fibres: (a) a hierarchical porous fibre [37], (b) a core/shell fibre [38], (c) an aligned fibre [39] and (d) a randomly oriented fibre [19].

sites for ion diffusion process. Table 1 summarised the recently reported NFs based electrodes for supercapacitor and their performance. However, NFs still suffer from a low specific capacitance, which is the major requirement for high-performance supercapacitors. Therefore, significant efforts have been devoted to achieving an electrochemical improvement of supercapacitors by incorporating NFs with pseudocapacitive materials, such as transition metal oxides (TMOs) and conducting polymers, (CPs) which undergo a fast and reversible faradaic reaction, resulting in a 10–100 times higher capacitance than NFs alone. Although several reviews have covered the development of transition metal oxide- and conducting polymer-based carbon fibre composites as supercapacitor electrodes [10,30–36], there is comprehensive review on TMO/CP-based fibres and their utilisation in the advancement of supercapacitor application.

This review mainly focuses on recent advances in TMO-, CP- and TMO/CP-based fibres as promising supercapacitor electrodes. The structural design, assembly method and electrochemical performance of the electrodes are also discussed. Firstly, we review recent progress in the development of TMO-based fibres using different kinds of TMOs. Secondly, significant advances achieved by incorporating CPs into the fibres are discussed in detail. Thirdly, the recent studies on the design and electrochemical performance of TMO/CP-based fibres are presented in this review. Finally, the limitations, future prospective and recommendations are also discussed towards improving the capacitive performance of current TMO/CP-based fibres based supercapacitors.

## 2. Supercapacitors and their mechanisms

Supercapacitors also known as ECs or ultracapacitors have attracted significant attention in energy sustainability due to their excellent electrochemical performance, that is, high specific capacitance, rapid charge/discharge rate, high specific power and long cycle life (>10<sup>5</sup> times) [58–62], which is incomparable to those of other energy storage

devices. Typically, two electrodes, an electrolyte and a separator are the required components to assemble a full-cell supercapacitor. The configuration of a full-cell supercapacitor can be either symmetric or asymmetric. Two electrodes are separated by a separator (filter paper, glassy paper, cellulose or polyacrylonitrile membrane), which has good ion permeability properties for ion transportation [63]. According to the energy storage mechanism, supercapacitors are classified into electrical double-layer capacitors (EDLCs), pseudocapacitors (PCs) and hybrid capacitors (HCs), as shown in Fig. 3. In general, EDLCs mainly employ carbon electrode materials, such as graphene, activated carbon, nano-architected carbon and carbon aerogels, for the accumulation of charge via reversible adsorption/desorption of ions at the electrode/electrolyte interface [64–67]. The charge/discharge process in EDLCs is equivalent to the dielectric behaviour of conventional capacitors as there is no faradaic reaction occurring during the energy storage process [68]. EDLC materials have been studied extensively owing to their high SSA [69], good electrical conductivity and excellent mechanical stability [70], but they suffer from a low specific capacitance [71]. The second group of supercapacitors is called pseudocapacitors (or redox capacitors) in which the energy is stored via a fast and reversible faradaic reaction at the surface of the active materials. Suitable materials for pseudocapacitors are thoroughly being investigated, as TMOs offer a relatively high specific capacitance [72] and superior specific energy [73] while CPs have a good intrinsic conductivity [72], thus making them unique candidates for high-performance supercapacitors. Unfortunately, CPs suffer from poor cycling-stability performance due to the repeated swelling and shrinking of the polymer chains during the doping/dedoping process [74–81]. For TMOs, the major drawback is the low conductivity, which greatly hinders them from reaching the high theoretical specific capacitance value. Due to the limitations of each material, many attempts have been made to fabricate HCs [18,19,21,22,82–85] that combine the advantages of the behaviours of both EDLCs and pseudocapacitors, enhancing the electrochemical performance. NFs

**Table 1**  
Comparison of electrochemical performance derived from NFs-based electrodes with different morphology.

Composite electrode	Composition	Capacitance	Specific energy	Stability performance (%)	Reference
Porous fibres					
Porous CNFs	Nafion/PAN (80:20)	210 F/g (60 F/cm <sup>3</sup> )	4 Wh/kg	–	[26]
Lignin CNFs	Mg(NO <sub>3</sub> ) <sub>2</sub> ·6H <sub>2</sub> O/lignin-PVP (2:1)	248 F/g	–	97 (1000 cycles)	[40]
Silicon carbide nanofibres membrane (SiC-NFMs)	PCS/PS in the xylene	189 F/g	–	91.7 (3000 cycles)	[41]
Nitrogen-enriched hierarchical porous carbon nanofibers (HPCNFs)	PAN/Mg (OAc) <sub>2</sub>	263 F/g	9.15 Wh/kg	94.2 (10,000 cycles)	[42]
Porous CNFs composites (NFCs)	PAN/PMHS	126.86 F/g	17 Wh/kg	–	[43]
1D hierarchical porous CNFs (HPCNFs)	PAN/DMF/THF	251 F/g	–	88 (5000 cycles)	[44]
Porous ultrafine CNFs ( <i>u</i> -CNFs)	PAN/PMMA	86 F/g	–	–	[45]
Core/shell fibres					
CNFs@PPy@rGO core shell fibres	PAN/DMF	92.57 F/g	–	86 (10,000 cycles)	[46]
Hierarchical core-shell Co <sub>3</sub> O <sub>4</sub> /graphene hybrid fibres	rGO fibres/Co(CH <sub>3</sub> COO) <sub>2</sub>	236.8 F/g (196.3 mF/cm <sup>2</sup> )	–	72.7 (10,000 cycles)	[47]
MnO <sub>2</sub> @PAA/PPy core-shell composite fibres	PAA/Mn(CH <sub>3</sub> COO) <sub>2</sub>	564 F/g	–	100 (5000 cycles)	[48]
Core-shell N-doped active CNFs@graphene (ACNFs@GR)	CNFs@GR/KOH (1:4)	552.8 F/g	17.1 Wh/kg	90 (2000 cycles)	[49]
Honeycomb manganese oxide@CNFs core shell nanocables (HMO@CNFs)	CNFs (core)/KMnO <sub>4</sub> (shell)	295.24 F/g	22.2 Wh/kg	96.4 (3000 cycles)	[50]
Hierarchical NiCo <sub>2</sub> O <sub>4</sub> -CNFs@Ni(OH) <sub>2</sub> core-shell nanofibres	PAN/PVP/Co(OAc) <sub>2</sub> /Ni(OAc) <sub>2</sub>	1925 F/g	–	87 (5000 cycles)	[27]
Aligned fibres					
1D aligned graphene fibres	Graphite:NaNO <sub>3</sub> :KMnO <sub>4</sub> (1:1:5)	279 F/g (340 F/cm <sup>3</sup> )	–	–	[51]
Robust vertically aligned carbon nanotube-carbon fibre paper (VACNT-CFP)	VACNT-CFP	6.1 mF/cm <sup>2</sup>	–	~110 (10,000 cycles)	[52]
Aligned carbon nanofibres/carbon fibre yarn (CFY@CNFs)	CFY@PAN NFs	62 mF/cm <sup>2</sup>	1.4 μW h/cm <sup>2</sup>	–	[53]
Oriented graphite fibres	SSP-PEDOT fibres	54.4 F/g	–	–	[28]
Random fibres					
Polyaniline-carbon nanofibres (PANI-CNFs)	10 wt% PAN in DMF/20 wt% sol-gel TEOS/DMF	234 F/g	32 Wh/kg	90 (1000 cycles)	[54]
CNFs with multilevel porous structure	10 wt% PVDF – 8 wt% PVP/20 wt% PVP	331 F/g	–	99.6 (10,000 cycles)	[55]
Activated porous carbon nanofibres/SnO <sub>2</sub> (APCNFs/SnO <sub>2</sub> )	PAN/Cu(Ac) <sub>2</sub> ·H <sub>2</sub> O/SnCl <sub>2</sub>	225.4 F/g	10.3 Wh/kg	~119.8 (2500 cycles)	[56]
Coal-derived carbon nanofibres (CCNFs)	PAN/PVP/coal (5:5:20 wt%)	299.4 F/g	–	93 (10,000 cycles)	[29]
Free-standing flexible carbon nanofibres	PVB/silica sol/phenolic sol	274 F/g	–	90 (5000 cycles)	[57]



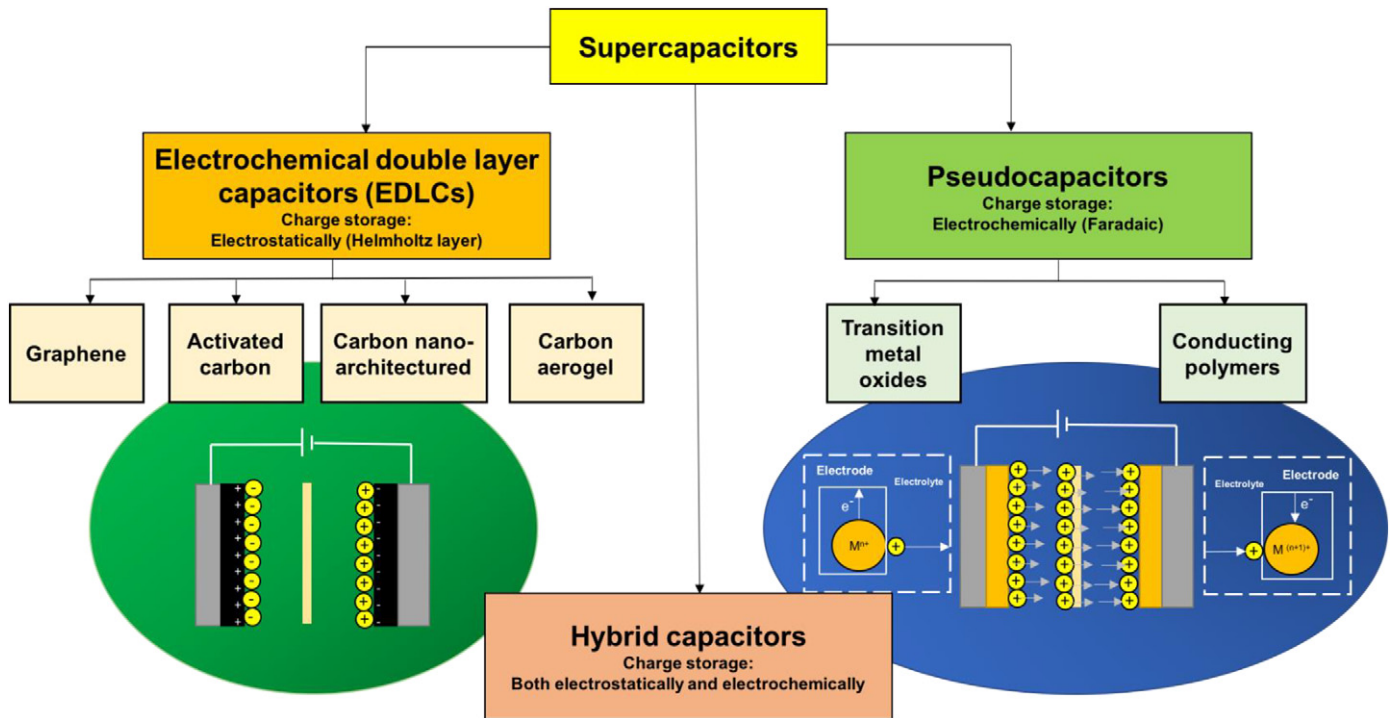


Fig. 3. Classification of supercapacitors.

have been commonly used in electrochemical applications as anodes, cathodes, separators and catalytic materials [17]. The adjustable diameter (micrometres to nanometers), high surface area and controllable pore size of NFs makes them useful in improving the electrochemical performance of electrodes.

### 3. Strategies for NFs fabrication

There are various methods for preparing NFs, namely, electrospinning (ES), wet spinning, dry spinning, solution blow spinning, gel spinning, centrifugal jet spinning, plasma-induced synthesis, chemical vapour deposition (CVD) and hydrothermal synthesis. However, some techniques are relatively complicated, time-consuming and expensive, which can limit the reproducibility of the as-prepared NFs. Thus, it is significant to develop a simple and time-saving route to fabricate NFs. The ES method has been widely adopted because it is straightforward, leads to tunable characteristics (diameter, morphology and composition) and can be scaled-up for industrial production [15]. Hence, the ES setup, the process of NFs production and the factors influencing the fibres' morphology are summarised below.

#### 3.1. Electrospinning

In general, there are three components required in a typical ES setup: a high-voltage power source (kV), a syringe pump, a spinneret with a metallic needle and a grounded fibre collector, as illustrated in Fig. 4. The ES setup is classified into two types of systems: the horizontal-position ES (dynamic mode) (Fig. 3a) and the vertical-position ES (static mode) (Fig. 3b). A syringe filled with a polymer solution or a melt is connected to the high-voltage source at the end of the needle containing a pendant droplet. A syringe pump is used to control the flow rate of the electrospun solution being ejected as fibres to the collector. The polymer droplet is electrostatically charged and elongated forming a Taylor cone shape from the hemispherical surface [86]. At a critical voltage, sufficient electrostatic force overcomes the surface tension of the polymer solution and a stable jet erupts from the spinneret to the oppositely charged

collector. The repulsive force between the charged jets becomes increases causing to bending instability and further elongates forming thinner fibres. Then, the jet slowly undergoes evaporation and solidification, producing continuous electrospun fibres. The viscosity of the polymer solution, applied voltage, flow rate and tip-collector distance are the major parameters which influence the morphology of the electrospun fibres [87]. Moreover, assembly of the fibres can be achieved using different types of collectors; for example, fibres with a web-like morphology are fabricated via a static collector, whereas non-woven fibres are produced using a cylindrical collector rotating drum [23].

#### 3.2. Carbon nanofibres

For supercapacitors based on the electric double layer (EDLC), electrode materials such as graphene, activated carbon, carbon aerogels, carbon nanofibres (CNFs) and carbon nanotubes (CNTs) exhibit remarkable features due to their stable electrochemical performance over long periods. Among these, CNFs have been regarded as one of the most promising candidates for supercapacitors, which can offer excellent electrical conductivity and thermal and mechanical stability as well as an increased SSA [88] and simple preparation [18,19,89]. In general, any polymer with carbon backbone can be used as electrospun CNF precursor; they can be classified into aqueous polymers (polyvinyl alcohol (PVA), poly(vinyl pyrrolidone) (PVP), poly(vinyl acetate) (PVAc) and polyethylene oxide (PEO)) and non-aqueous polymers (polyacrylonitrile (PAN), poly(vinylidene fluoride) (PVDF), polylactic acid (PLA), polymethacrylate (PMMA) and polyvinylchloride (PVC)) [17,20–22,83]. However, PAN was found to be the most common electrospun CNF precursor owing to its outstanding properties, such as high carbon yield (of >50%) [90], flexibility [72] and environmental friendliness [91]. CNFs can be prepared in two steps including stabilisation followed by a carbonisation process. Firstly, the electrospun NFs are placed in a tube furnace and stabilised in air at a temperature between 250 and 300 °C. At this stage, the polymer is converted into a ring structure (ladder compound), which helps to retain the fibrous structure at a higher temperature. Then, the stabilised fibres are subjected to carbonisation in an inert atmosphere (at a temperature above 500 °C)

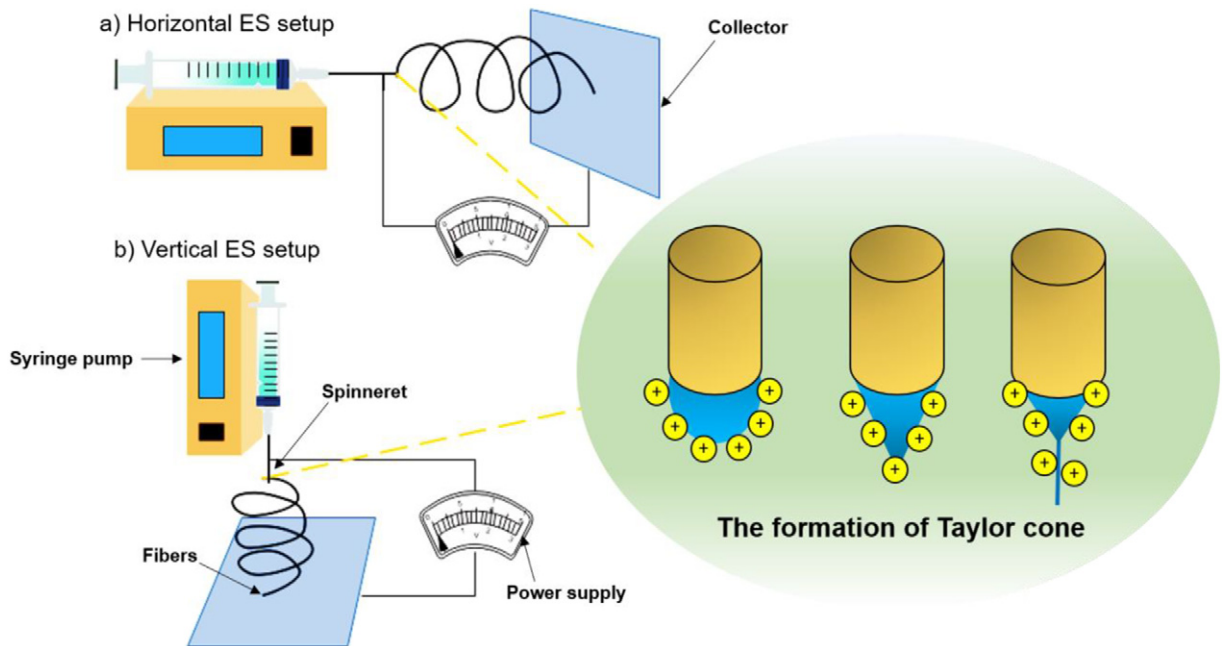


Fig. 4. Schematic diagram of a typical ES system showing the formation of Taylor cone with a stable jet: (a) horizontal setup and (b) vertical setup.

and transformed into graphite-like CNFs, as shown in Fig. 5. Moreover, most of the non-carbon elements ( $\text{H}_2\text{O}$ ,  $\text{CO}_2$ ,  $\text{NH}_3$ ,  $\text{HCN}$ ,  $\text{CO}$  and  $\text{N}_2$ ) are eliminated during this process [23], resulting in smaller diameter of CNFs, larger accessible surface area and better conductivity. Moreover,

the development of a porous structure in the CNFs (i.e. micropores, mesopores and macropores) has been widely studied for flexible supercapacitors (FSCs). Feng et al. [92] reported that microporous CNFs (<2 nm) can partially block electrolyte ions into the micropores during

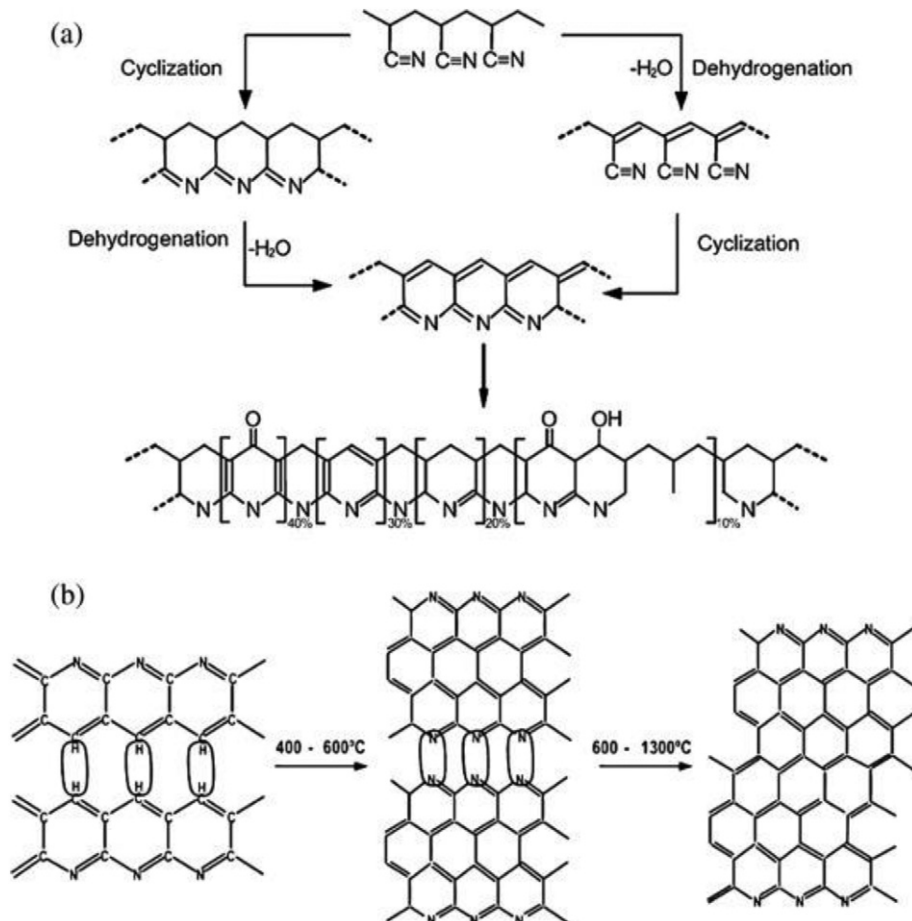


Fig. 5. Changes in the molecular structure of PAN to CNFs by the: (a) stabilisation [96] and (b) carbonisation [97] processes.

the charge/discharge process [93], leading to an increase in the charge transfer resistance ( $R_{ct}$ ). To overcome this ionic diffusion problem, mesoporous (i.e. 2–50 nm) CNFs are preferable to provide more void spaces for ion migration, thus exhibiting a superior electrochemical performance [94]. Interestingly, micro/mesoporous CNFs originated from PAN fibres, silica template and KOH activation possess a SSA up to 1796 m<sup>2</sup>/g, which promotes the fast transport/diffusion of electrolyte ions, displaying a high specific capacitance of 197 F/g [95]. Although the capacitance of porous CNFs has been improved, extensive studies have been performed to control the pore size within the CNFs for high-performance supercapacitors.

#### 4. Transition metal oxides

In developing advanced high-performance energy storage systems, TMOs have attracted vast attention as pseudocapacitor electrodes due to their excellent specific energy output compared with EDLC materials. Several TMOs, such as ruthenium oxide (RuO<sub>2</sub>), manganese oxide (MnO<sub>2</sub>), nickel oxide (NiO), cobalt oxide (Co<sub>3</sub>O<sub>4</sub>) and vanadium oxide (V<sub>2</sub>O<sub>5</sub>), are commonly used in supercapacitors owing to their high theoretical specific capacitance from the faradaic charge transfer process [98–103]. Fig. 6 shows the theoretical capacitances of different TMOs obtained from cyclic voltammograms. Unfortunately, the factors that hinder achieving a high specific capacity in TMOs are the easy agglomeration of TMOs at high mass loading [7], poor cyclability and conductivity properties [104]. Thus, the incorporation of conductive materials, such as EDLC materials, with the TMOs can considerably enhance the ionic and electrical conductivity by the synergistic effect of different components [105].

##### 4.1. Ruthenium-oxide-based fibres

Ruthenium oxide (RuO<sub>2</sub>) is regarded as an important electrode for oxide-based supercapacitors with excellent capacitive behaviour because it has a high theoretical specific capacitance (in the range of 750–2000 F/g) [107], a good electrical conductivity and a better rate capability [108]. Although the preparation of RuO<sub>2</sub> is expensive, this oxide can be considered as a potential supercapacitor material that can enhance the specific energy compared to EDLC and other CP-based electrodes [109]. Nevertheless, the superior electrochemical performance of RuO<sub>2</sub> is hampered by the agglomeration of RuO<sub>2</sub> particles during the charge/discharge process [110].

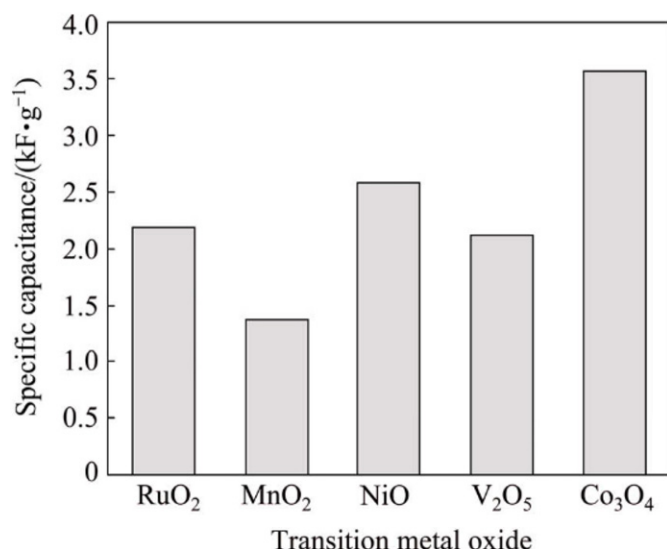


Fig. 6. Comparison of the theoretical specific capacitances of different TMOs [106].

The introduction of one-dimensional (1D) nanostructures such as CNFs, which have a large SSA [88] as well as good conductivity and mechanical stability [19], could improve the efficiency of RuO<sub>2</sub>, leading to an efficient charge propagation in the composite. Coaxial nanostructures of amorphous ruthenium oxide (RuO<sub>x</sub>)/graphitic nanofibres (GNFs) were synthesised by Jhao et al. [111] via CVD and subsequent electrodeposition of RuO<sub>x</sub>. The obtained coaxial RuO<sub>x</sub>/GNF nanostructures exhibited a macroporous structure, which allowed more electrolyte ions to diffuse into the inner active sites, delivering a high areal capacitance of 53.76 mF/cm<sup>2</sup> at 50 mV/s with good cycling stability (83% capacitance retention) over 5000 cycles. Two pair of redox peaks can be observed in the CV curve of RuO<sub>x</sub>/GNF, which can be attributed to the Faradaic reaction behaviour of RuO<sub>x</sub>, contributing to the high areal capacitance. The nanostructured pores in the carbon matrix can be constructed by adding a sacrificial component, which will be decomposed during the carbonisation process. Kim et al. [112] reported the fabrication of RuO<sub>2</sub> incorporated with highly mesoporous activated carbon nanofibres (RuPM-ACNFs) via electrospinning of two polymer blends, PAN and poly(methyl methacrylate) (PMMA), followed by an activation process. The optimal PAN/PMMA blend ratio (70:30) led to the highest specific energy of 24 Wh/kg at a specific power of 400 W/kg with small semicircle ( $R_{ct} = 1.07 \Omega$ ), which was mainly attributed to the abundance of mesopores that can provide active sites for rapid ion transportation.

Furthermore, RuO<sub>2</sub>-based ternary hybrid composites have also received intensive interest for high-performance supercapacitors. Balan et al. [113] obtained a specific capacitance of 1060 F/g (at a scan rate 20 mV/s over a voltage window of 1.3 V) using a dual-wall carbon nanofibre–RuO<sub>2</sub>–poly(benzimidazole) (PBI) (CNFs–RuO<sub>2</sub>–PBI) material (Fig. 7). This ternary hybrid electrode was fabricated by embedment of RuO<sub>2</sub> nanoparticles (NPs) on functionalised hollow carbon nanofibres (f-CNFs) via a modified polyol process, followed by the incorporation of phosphoric-acid-doped PBI. As shown in the transmission electron microscopy (TEM) image, a thin phosphoric acid doped poly(benzimidazole) (PBI-Bul) film was uniformly wrapped on the RuO<sub>2</sub> NPs without aggregation, which can reduce the charge transfer resistance at the electrode/electrolyte interface. Unfortunately, the sample preparation is relatively complicated and time-consuming, which is not suitable for large-scale production. Therefore, Kim et al. [114] proposed a simple and fast preparation of RuO<sub>2</sub>/ACNF by electrospinning and activation. Interestingly, the as-prepared electrode (with 20% RuO<sub>2</sub> concentration) possessed an improved electrical conductivity (4.5 S/cm) with large SSA (675 m<sup>2</sup>/g), leading to a high specific capacitance of 530 F/g at 20 mV/s.

##### 4.2. Manganese oxide-based fibres

MnO<sub>2</sub> has emerged as an excellent faradaic material, which can be used as an alternative TMO (replacing RuO<sub>2</sub>) due to its good environmental compatibility [115], high theoretical specific capacity (1370 F/g) [116–118], extended operating potential and cost-effectiveness [119]. However, the only limitations of MnO<sub>2</sub> for commercial applications are its poor ionic (10<sup>-13</sup> S/cm) and electrical (10<sup>-5</sup>–10<sup>-6</sup> S/cm) conductivities [120], which restrict its practical capacitance and rate capability. To date, the rational design of MnO<sub>2</sub> nanoarchitectures has been considered as a promising way to make full use of the pseudocapacitance of MnO<sub>2</sub> and the large accessible surface area of conductive fibre materials.

Yang et al. [121] reported an ultrafine manganese oxide–carbon nanofibre (MnO<sub>x</sub>-CNF) composite prepared through the pyrolysis of a metal-organic framework containing Mn, a Zn precursor and trimesic acid (H<sub>3</sub>BTC) (Mn–ZnBTC). The non-aggregated and well-dispersed morphology of the MnO<sub>x</sub>-CNF delivered a capacitance of up to 179 F/g and kept good cycling durability of 98% over 5000 cycles. These results can be ascribed to the enhanced contact area between MnO<sub>2</sub> and the CNFs, which leads to good synergistic effects for superior electrochemical performance. Chen et al. [122] applied the electrodeposition method for synthesising a MnO<sub>2</sub>@carbon fibre paper (MnO<sub>2</sub>@CFP) and further



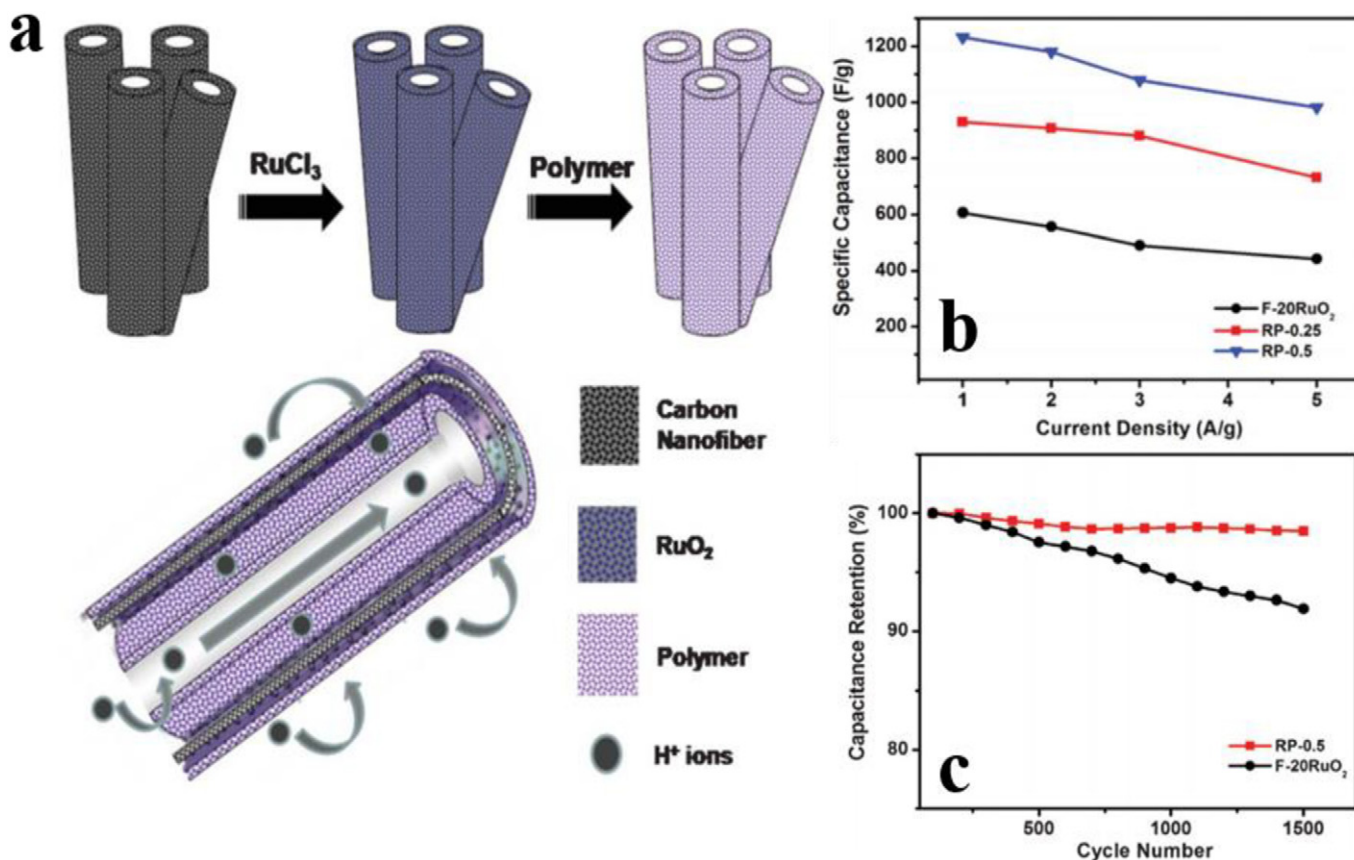


**Fig. 7.** (a) Schematic illustration of the synthesis of dual-wall carbon nanofibre–RuO<sub>2</sub>–poly(benzimidazole) (PBI) (CNFs–RuO<sub>2</sub>–PBI). (b) Specific capacitance of F-20RuO<sub>2</sub>, RP-0.25, RP-0.5 at different current densities (1 to 5 A/g). (c) Stability performance of RP-0.5 and F-20RuO<sub>2</sub> over 1500 cycles at current density 1 A/g [113].

treated it with a potassium sulphate (K<sub>2</sub>SO<sub>4</sub>) solution by the hydrothermal method. The treated MnO<sub>2</sub>@CFP showed a gravimetric capacitance value of 281.9 F/g and an improved rate capability compared to that of untreated MnO<sub>2</sub>@CFP, as K<sub>2</sub>SO<sub>4</sub> can preserve the ramdellite structure of Mn (MnO<sub>2</sub>) during the hydrothermal process. Likewise, a higher specific capacitance of 473 F/g can be achieved using mesoporous MnO<sub>2</sub> core-shells coated on vertically aligned carbon nanofibres (MnO<sub>2</sub>/VACNFs) [123] due to the short diffusion distance of the electrolyte ion across the MnO<sub>2</sub> shell, which is less than ~10 nm. Besides, the fabrication of CNFs using disposable and low-cost bamboo chopsticks has been studied by Wen et al. [124]. MnO<sub>2</sub> NPs (20–50 nm) were electro-deposited on the obtained carbon-fibre sheets (CFSs), providing a high specific capacitance of 375 F/g at 1 A/g, a remarkable specific energy (i.e. 11.0 Wh/kg at a specific power of 529 W/kg) and a good long-term cycle stability (99.2% capacitance retained after 5000 cycles). The superior electrochemical performance of obtained CFSs/MnO<sub>2</sub> could be ascribed from the synergistic effect of faradic and EDLC charge storage mechanism and large electroactive sites which offers fast diffusion and migration of electrolyte ion.

Moreover, the development of core-shell fibres have been extensively investigated to enhance the electrochemical reactivity in hybrid supercapacitors; for instance, Pech and Maensiri [125] prepared carbon-manganese oxide composite fibres (C/MnO<sub>x</sub>) through a core-shell electrospinning approach, where an individual PAN solution was used as the core solution while a PAN–manganese nitrate (Mn(NO<sub>3</sub>)<sub>2</sub>) blend was used as the shell solution. Benefitting from the EDLC and pseudocapacitive characteristics of carbon and MnO<sub>x</sub>, the C/MnO<sub>x</sub> hybrid achieved a large SSA (701 m<sup>2</sup>/g), thus improving the specific capacitance up to 213.7 F/g in 6 M KOH. The capacity of the as-synthesised electrode was retained efficiently (~97%) after 1000 charge/discharge cycles. Furthermore, Zhou et al. [126] presented a simple approach to synthesise

free-standing MnO<sub>2</sub> nanoflakes/porous carbon nanofibres (PCNFs) (MnO<sub>2</sub>/PCNFs) through one-step electrospinning followed by in-situ deposition, as shown in Fig. 8. The scanning electron microscopy (SEM) image revealed that the MnO<sub>2</sub> nanoflakes are vertically grown on the exterior surface of the PCNFs, contributing to a large surface area between MnO<sub>2</sub> and the electrolyte ions. The as-formed MnO<sub>2</sub>/PCNF possessed a high degree of mesoporosity and a high SSA (1814 m<sup>2</sup>/g), with 92.3% of the initial capacitance being maintained after 4000 cycles. However, the EIS result revealed that PCNF showed lower charge transfer resistance as compared with MnO<sub>2</sub>/PCNF which mainly corresponded to the high electronic conductivity induced by the electrode. Furthermore, Xu et al. [127] reported the rational design of hierarchical hollow MnO<sub>2</sub> nanofibres via the hydrothermal method. Brunauer–Emmett–Teller (BET) results demonstrate that the surface area of the hollow MnO<sub>2</sub> nanofibres was 195.1 m<sup>2</sup>/g, with an average mesopore size of ~3.9 nm which can provide numerous available active sites for electron transfer. Moreover, it is worth noting that the specific capacitance of the hollow MnO<sub>2</sub> nanofibres can be effectively retained from 291 to 213 F/g (at a current density of 1 to 10 A/g), demonstrating excellent electrochemical reversibility. It can be observed that all galvanostatic charge/discharge curves are approximately triangular and symmetrical, suggesting an ideal capacitive behaviour and reversibility. The utilisation of heteroatoms such as boron, which act as electron acceptors/dopants, has been recently studied to enhance the electrochemical capacitance of carbon materials through its pseudocapacitive effect.

Yang and Kim [128] employed MnO<sub>2</sub> to hybridise with boron-enriched PAN/pitch-based CNFs (PPBMn) via one-step electrospinning followed by carbonisation. This work highlighted that both boron and MnO<sub>2</sub> provide a low-resistance pathway for electron transport and more electrochemically active sites for the redox reaction. The resultant



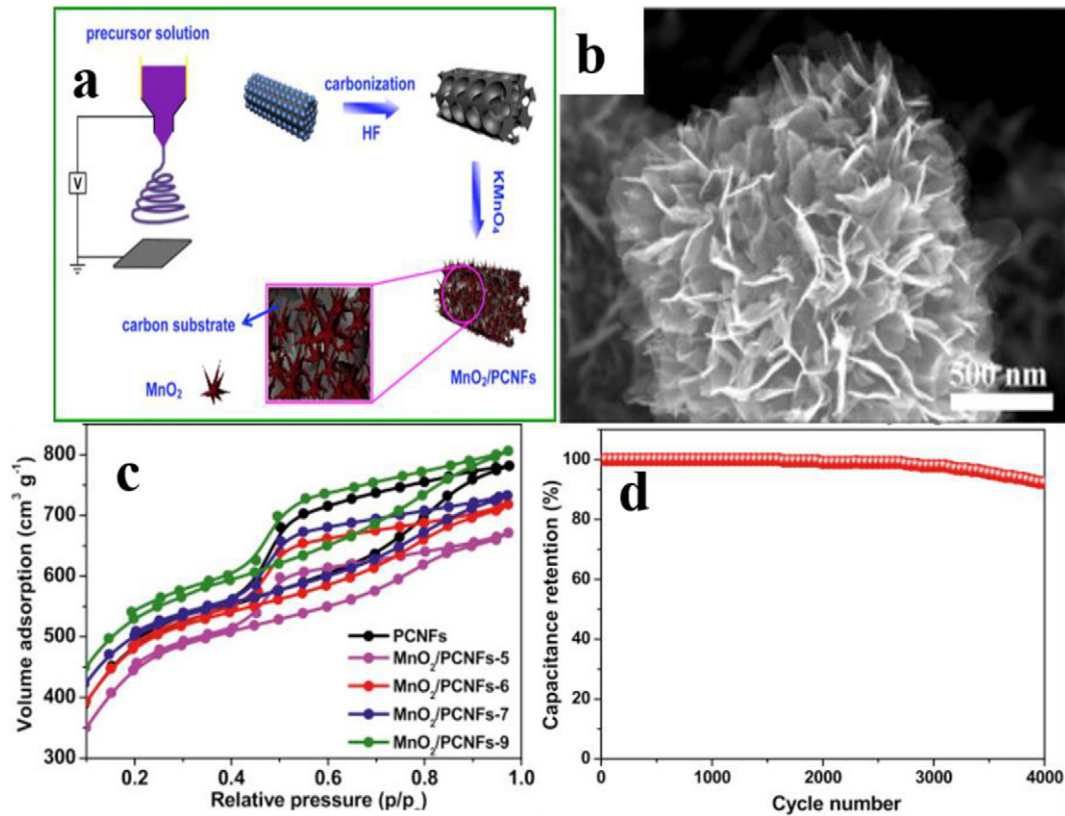


**Fig. 8.** (a) Schematic illustration of the synthesis of MnO<sub>2</sub>/PCNFs. (b) SEM image of MnO<sub>2</sub>/PCNFs-6. (c) Nitrogen adsorption/desorption isotherms for PCNFs and MnO<sub>2</sub>/PCNFs with different weight ratio of KMnO<sub>4</sub> and PCNFs [126]. (d) Long-term stability MnO<sub>2</sub>/PCNFs-6 electrode over 4000 cycles at current density 0.5 A/g.

PPBMn, with an SSA of 718 m<sup>2</sup>/g, delivered a high specific capacitance of 208 F/g with a maximum specific energy of 25.66 Wh/kg. Additionally, Chi et al. [129] found that boron doping also increases the growth rate of MnO<sub>2</sub> crystallites through a hydrogen bond, giving a specific capacitance of 364.8 F/g at a scan rate of 2 mV/s, which is substantially higher than that of the undoped electrode (305 F/g). However, boron-doped MnO<sub>2</sub> exhibited poor cycling stability (80.4% over 900 cycles), which is probably caused by Mn<sup>2+</sup> dissolution or a collapse of the inner structure. The combination of EDLC materials with MnO<sub>2</sub>-based fibres can eventually overcome the shortcomings of pseudocapacitive materials by boosting a high electrical conductivity and increasing the number of electrochemically active sites for rapid ion diffusion. For example, Lee and Kim [130] fabricated a supercapacitor electrode comprising MnO<sub>2</sub>/hierarchical porous carbon nanofibres/graphene (MnO<sub>2</sub>/HPCNFs/G) through simple approaches, namely, through electrospinning and a thermal process. In this case, graphene, with its good specific power and rate capability properties, provides good support for the uniform distribution of MnO<sub>2</sub> on HPCNFs/G, which can reduce the charge diffusion resistance, as reflected by the excellent electrochemical behaviour of the resulting material. MnO<sub>2</sub>/HPCNFs/G endowed a great specific capacitance of 210 F/g and the quasi-rectangular CV shape was retained even at high scan rates (10–100 mV/s), leading to excellent electrochemical reversibility.

Sliwak and Gryglewicz [131] reported high-voltage asymmetric supercapacitors (ASCs) based on activated carbon (AC) as the negative electrode and manganese oxide/oxidised carbon nanofibres (MnO<sub>2</sub>/CNF<sub>ox</sub>) as the positive electrode. The MnO<sub>2</sub>/CNF<sub>ox</sub>//AC ASCs showed a wide potential window of 0–2.4 V, maximum specific energy of 24.8 Wh/kg at a specific power of 100 W/kg and a good stability performance (92.4%) after cycling for 5000 times. Moreover, the assembled reduced graphene oxide–carbon nanofibres–manganese carbonate (positive electrode) and the reduced graphene oxide

(negative electrode) (RGO-CNFs-MnCO<sub>3</sub>//RGO) in 1 M Na<sub>2</sub>SO<sub>4</sub> aqueous electrolyte also presented a stable cyclability performance, with 97% retention even after 1000 cycles at a voltage cell of 2.0 V. Wang et al. [132] has designed δ-MnO<sub>2</sub> nanofibres/single-walled carbon nanotubes (δ-MnO<sub>2</sub>/SWCNTs) through vacuum filtration. Using polyvinyl alcohol and potassium hydroxide (PVA-KOH) as the electrolyte, the flexible all-solid-state δ-MnO<sub>2</sub>/SWCNT (with a high SSA) showed a higher areal capacitance (of 964 mF/cm<sup>2</sup>) as compared to single SWCNT and δ-MnO<sub>2</sub> films. These results could be attributed to the superior properties of the SWCNTs, which provide a high surface area and a good electrical conductivity to the δ-MnO<sub>2</sub>/SWCNT hybrid electrodes, thus increasing the composite's conductivity up to 81.11 S/cm.

Recent advances in mixed TMO-based fibres has garnered tremendous attention in supercapacitor applications. Radhamani et al. [133] reported the synthesis of ZnO@MnO<sub>2</sub> core-shell nanofibres (ZnO@MnO<sub>2</sub> NFs) as a potential cathode for ASCs. The uniform distribution of MnO<sub>2</sub> nanoflakes on a ZnO-NF surface (as observed in TEM images) allowed the shortening of the ion-diffusion path, resulting in an increased overall capacitance of 907 F/g in a three-electrodes configuration. Furthermore, the fabricated ZnO@MnO<sub>2</sub> NFs also succeeded to light a commercial red light-emitting diode (LED) after being fully charged up to 2 V. Meanwhile, Iqbal et al. [134] electrospayed MnO<sub>2</sub> particles on Fe<sub>3</sub>O<sub>4</sub>@CNFs (Fe<sub>3</sub>O<sub>4</sub>@CNF<sub>Mn</sub>) to form a highly flexible supercapacitor electrode. Gold-sputtered polyethylene terephthalate (PET) and sodium sulfate/poly(vinyl alcohol) (Na<sub>2</sub>SO<sub>4</sub>/PVA) served as the current collector and separator, respectively, to evaluate the feasibility properties of the obtained electrode. The combination of microporous- and mesoporous-structured CNFs delivered a high specific capacitance (~306 F/g) and enabled the perfect retention of the electrochemical performance at different bending angles (0–180°). This makes them great candidates for lightweight and flexible energy storage.

### 4.3. Nickel oxide-based fibres

Nickel oxide (NiO) is regarded as a promising supercapacitor electrode compared with other TMOs because it offers a high theoretical capacitance (2584 F/g) [135], a high surface area [136], non-toxicity and low manufacturing costs [137]. Different NiO nano-morphologies, including nanoribbons [138], nanosheets [139], nanowires [140], nanoflakes [141] and NPs [142], can be simply prepared via hydrothermal, chemical immersion, solvothermal, microwave hydrothermal and electrodeposition processes, respectively. Recently, researchers have focused on developing sustainable fibres with a high SSA incorporated with a modified NiO structure that provides great benefits for the rapid transfer of electrons. Zhu et al. [143] proposed the decoration of three-dimensional (3D) NiO nanowalls, via a hydrothermal process, combined with a post-annealing treatment (at 600 °C) that assisted the uniform growth of CNFs on metal wires (MWs) through a CVD process. The enhancement of the substrate surface from the pre-deposited 3D NiO nanowalls showed a remarkable areal capacitance of 12.5 mF/cm<sup>2</sup> with an excellent cyclability performance (91%) after 3000 cycles due to the high capacity properties contributed from the CNFs. In order to further verify the property of CNFs/MW (3D) NiO as high-performance supercapacitor, two devices were assembled in series to light a light emitting diode (LED). Undoubtedly, the light emitting diode can be successfully lit, showing their potential application in wearable and portable electronics. In addition, the in-situ fabrication of dilute NiO/CNFs through direct pyrolysis of a metal-organic framework (MOF) containing Ni and Zn has been studied by Yang et al. [135]. MOFs are a new class of porous, crystalline materials constructed by covalent coordination between metal ions/clusters and organic molecules, where the conductivity and porosity of the final product can be tuned by varying the feed ratio of the metal precursors [144]. The unique mesoporous structure of NiO/CNFs leads to an excellent rate capability, as the specific capacitance only drained 29% from its initial capacitance (from 234 to 167 F/g), even at high scan rates. Additionally, a great dispersion of NiO onto the CNF surface led to a high specific energy (of 33.4 Wh/kg) with a negligible voltage drop (IR drop), indicating a good rate performance and a low internal resistance, respectively. Recently, hollow tube nanofibres containing NiO sheets were successfully introduced by Ren et al. [136] using the electrospinning technique with the inclusion of citric acid. The prepared NiO/citric acid nanofibres showed an enlarged SSA, with diameters ranging between 100 and 120 nm, and displayed a promising electrocapacitive behaviour with a high specific capacitance (336 F/g) compared to NiO nanofibres without citric acid. Moreover, the formation of a hollow structure could also provide a short electron-diffusion pathway, contributing to a low charge transfer resistance, which can be estimated to be about 0.23 Ω. The disadvantages of the poor intrinsic conductivity of NiO can be alleviated by designing porous NiO nanostructures, which can help to maximise the active surface area. For instance, Zang et al. [145] reported the synthesis of porous NiO nanofibres through a hydrothermally assisted process followed by calcination for application in a supercapacitor. The as-synthesised NiO nanofibres possessed a high specific capacitance (of 884 F/g at a current density of 0.5 A/g), with the capacitance fading only by 13% after 1000 cycles due to the unique morphology of the porous NiO nanofibres, which led to a rapid electron transfer during the faradaic process. Besides, Kundu and Liu [146] adopted a simple approach to grow porous NiO nanofibres on a nickel foam (NiO-NFs/Ni) by electrospinning and subsequent thermal annealing. This binding-free electrode revealed a specific capacitance of 737 F/g and showed a fascinating long-term stability performance up to 8000 cycles. These advanced capacitive performances could be elucidated from the porous interconnected network of NiO-NFs, which effectively attached on the Ni foam, thus improving the rate of the ion diffusion process through effective utilisation of the active material. Meanwhile, NiO NPs dispersed throughout porous N-doped CNFs (NiO/PCNFs) prepared by Li et al. [147] generated strong synergistic effects between the NiO NPs and the PCNFs, which resulted in a significantly enhanced specific capacitance (850 F/g at 1 A/g) in 6 M KOH

electrolyte. The NiO NPs were homogeneously distributed along the entire fibres and pores of various sizes were observed due to the evolution of different gases (CO, CO<sub>2</sub>, H<sub>2</sub>O and NH<sub>3</sub>), caused by the decomposition of dicyandiamide (DCDA). The presence of non-aggregated NiO as well as the formation of pores on the PCNFs are beneficial, providing a continuous charge transport pathway that results in high capacitive properties and a small ion-diffusion resistance. In addition, this work proves that a higher nitrogen content, doped on the PCNFs (NiO/PCNFs-0.75), can lead to a superior rate capability (about 88% capacitance retention) as well as to an improved cycling stability (96.7%) after 10,000 cycles (Fig. 9).

### 4.4. Cobalt oxide-based fibres

In recent years, cobalt oxide (Co<sub>3</sub>O<sub>4</sub>) has been particularly appealing as an ideal pseudocapacitor material, owing to its exceptionally good redox properties [148], theoretically high specific capacitance (3560 F/g) [149] and simple synthesis, which potentially can substitute the utilisation of high-cost and non-environmentally friendly RuO<sub>2</sub>. The electrochemical properties of Co<sub>3</sub>O<sub>4</sub> are greatly dependent on the structural morphology of the material and the electronic states of the metal (Co<sup>3+</sup> or Co<sup>2+</sup>) [150], and therefore, diverse strategies have been dedicated to developing various forms of Co<sub>3</sub>O<sub>4</sub> nanocomposites to achieve a better charge storage performance. Iqbal et al. [151] improved the electrical conductivity and electrochemical stability of Co<sub>3</sub>O<sub>4</sub> NPs by combining them with hierarchical porous CNFs to form a hybrid supercapacitor. A CNF-Co hybrid composite was prepared by cost-effective electrospinning followed by carbonisation, essentially leading to a high surface area (of 483 m<sup>2</sup>/g) and enhanced electrolyte-ion penetration. This work has shown an outstanding specific capacitance of 911 F/g in 1 M H<sub>2</sub>SO<sub>4</sub> electrolyte, retaining 78% of the initial capacitance over 1000 cycles. The inclusion of binary metal oxides, such as CoMnO<sub>2</sub>, in the composite electrode is an alternative way to enhance the electrochemical performance further. Kim et al. [152] prepared a Mn-Co oxide using vapour-grown carbon nanofibres (VGCNFs) (CoMnO<sub>2</sub>/VGCNFs) on a Ni-foam substrate via thermal decomposition of the metal-oxide precursors and annealing of the VGCNFs. The researchers reported a high specific capacitance of 630 F/g at a scan rate 5 mV/s which can be ascribed from the contribution of VGCNFs that provide multi-dimensional electron transport pathways, easy access to electrolyte, and minimised transport distance between the surface of cobalt-manganese oxide and bulk electrolyte. A better electrical contact between CoMnO<sub>2</sub>/VGCNFs and the Ni foam also led to a high capacitance retention (95%) after 10,000 cycles. In addition, 1D spinel CoMn<sub>2</sub>O<sub>4</sub> (CMO) porous nanofibres have been successfully synthesised by one-step electrospinning for solid-state supercapacitors [153]. Interestingly, encircled areas representing pores/gaps were formed between the spherical CMO particles, which can act as ion-buffering reservoirs. The unique architecture of CMO, which is composed of voids/gaps, decreased the ion-diffusion resistance (6.13 Ω), leading to a superior specific energy of 75 Wh/kg at a specific power of 2000 W/kg. Interestingly, a red-coloured light emitting diode connected to the solid-state CMO can maintain lighting for 5 min after being charged to 2.0 V, which is attributed to the high output voltage.

### 4.5. Vanadium oxide-based fibres

Among the redox-active TMOs, vanadium oxide/pentoxide (V<sub>2</sub>O<sub>5</sub>) is considered to be a promising pseudocapacitive electrode owing to its various oxidation states (V<sup>2+</sup> to V<sup>5+</sup>), unique layered structure [154] and wide potential window [155]. Composite fibres based on V<sub>2</sub>O<sub>5</sub> and carbonaceous materials are currently being studied for supercapacitors. Thangappan et al. [156] fabricated electrospun GO/V<sub>2</sub>O<sub>5</sub> nanofibres by the electrospinning method and the diameter of the fibres shrunked from 200 to 90 nm after annealing at 550 °C, giving a highly porous GO/V<sub>2</sub>O<sub>5</sub> structure with a rough surface. The diffusion of K<sup>+</sup> ions from

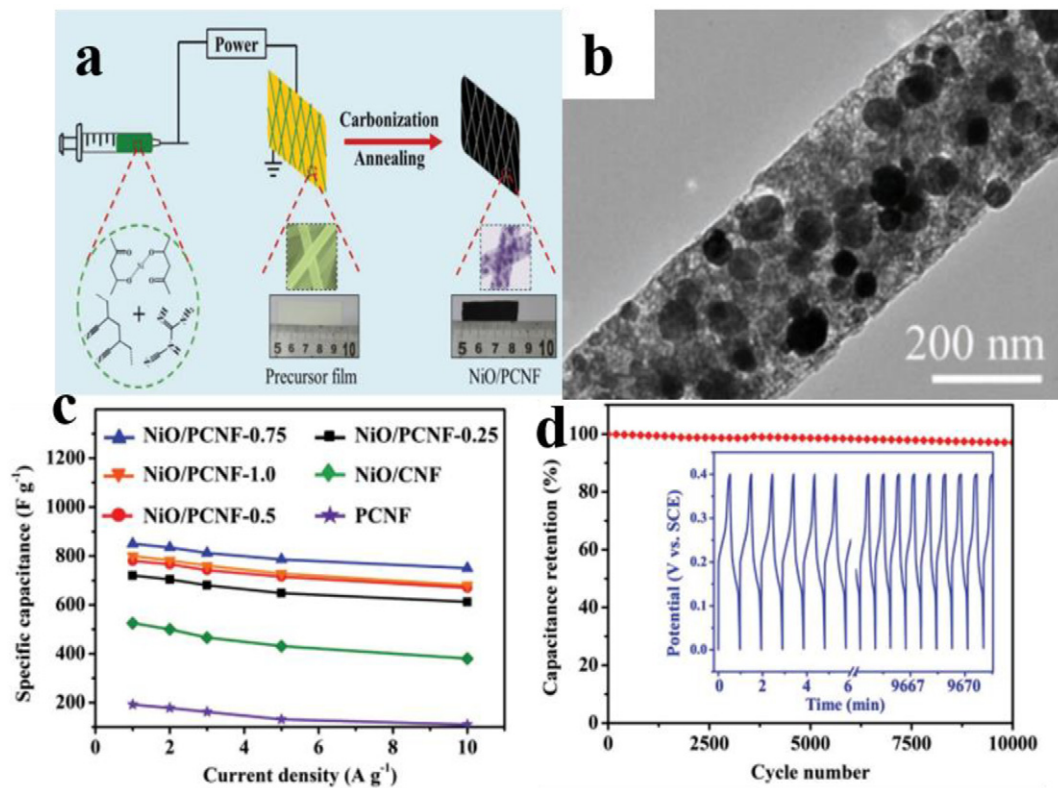


**Fig. 9.** (a) Schematic illustration of the synthesis of a free-standing NiO/PCNF composite film. (b) TEM image of NiO/PCNF-0.75. (c) Specific capacitance of NiO/PCNF-0.25, NiO/PCNF-0.5, NiO/PCNF-0.75, NiO/PCNF-1.0, NiO/CNF and PCNF free-standing electrodes versus the current density. (d) Cyclic stability of NiO/PCNF-0.75 at a charge/discharge current density of 10 A/g for 10,000 cycles (the inset refers to the charge/discharge curves), about 96.7% of the specific capacitance was retained [147].

the electrolytic layer into the pores of the GO/V<sub>2</sub>O<sub>5</sub> nanofibres is greatly facilitated by this unique morphology. Using 2 M KOH as the electrolyte, the specific capacitance of the GO/V<sub>2</sub>O<sub>5</sub> nanofibres was calculated to be 453.82 F/g at 10 mV/s, which is higher than those of the individual GO and V<sub>2</sub>O<sub>5</sub> components. However, the specific capacitance of GO/V<sub>2</sub>O<sub>5</sub> nanofibres gradually decreases with increasing scan rates, which could be ascribed to the limited ion incorporation into active electrode as only the outer surface is utilised during charging/discharging process. The enhancement in capacitance could also be attributed to the good conductivity and high surface area of graphene oxide. Kim et al. [157] applied both the electrospinning and carbonisation approaches to fabricate V<sub>2</sub>O<sub>5</sub>/CNFs (V<sub>2</sub>O<sub>5</sub>/CNFCs). In this work, different V<sub>2</sub>O<sub>5</sub> loadings (5, 10 and 20 wt%) were studied to control the microporous structure of CNFCs. The composite fibre containing V<sub>2</sub>O<sub>5</sub>-20 exhibited a high specific capacitance of 150 F/g and remarkable specific energy of 18.8 Wh/kg, which derives from the large interfacial area between the CNFCs and V<sub>2</sub>O<sub>5</sub>. However, the highest specific capacitance (739 F/g at 0.5 A/g) of amorphous V<sub>2</sub>O<sub>5</sub> doped with multichannel CNFs (VMCNFs) was reported by Huang et al. [158] using similar methods. A good synergistic effect between the high capacitance of V<sub>2</sub>O<sub>5</sub> and the enlarged SSA of MCNFs is responsible for the superior electrochemical properties. The addition of V<sub>2</sub>O<sub>5</sub> in multichannel CNFs could also improve the electrode-electrolyte interfacial area which can be observed from the decreasing in charge transfer resistance (0.27 Ω). Moreover, the development of mixed-TMO fibre composites (containing two metal oxides or bimetallic oxides) has attracted the interest of researchers due to their multiple oxidation states compared to single-metal oxides, thus contributing to the enhancement of the specific capacitance and cyclability performance [159]. The electrochemical performance of CNFs intercalated with bimetallic vanadium and copper oxides, denoted as Cu<sub>x</sub>O-V<sub>2</sub>O<sub>5</sub>/CNFs, was explored by adjusting the mass ratio of the vanadium and copper precursors [160]. According to the GCD results, the specific capacitance of the composite was as high as 867.2 F/g at a

current density of 0.5 A/g using an optimal mass ratio of vanadium and copper (10:1). Furthermore, the decrease in the solution resistance for Cu<sub>x</sub>O-V<sub>2</sub>O<sub>5</sub>/CNFs (0.22 Ω) is also attributed to the enhanced charge capacity of the bimetallic oxides. The electrochemical performances of TMO-based fibres for supercapacitor are summarised in Table 2.

## 5. Conducting polymers

CPs are widely studied as pseudocapacitor materials where the charges are stored under fast and reversible redox reactions at the surface and bulk of the electrode. CP electrode materials, including polyaniline (PANI), polypyrrole (PPy) and poly(3,4-ethylenedioxythiophene) (PEDOT), exhibit a maximum theoretical specific capacitance of 1000 F/g (100–400 μF/cm<sup>2</sup>), which is about two times higher than that of EDLCs [13]. In general, the excellent conductivity of CPs arises from the delocalisation of electrons along the conjugated polymer backbone, allowing electron transport in the doped state [22]. Moreover, the intrinsic conductivity of CPs can be changed from their chemical structure using economical ways, compared with TMOs [161]. Table 3 summarises the conductivities of different types of CPs and their chemical structures. CPs can be synthesised by chemical polymerisation or electropolymerisation of the corresponding monomers [162]. Despite the advantages of CPs, such as high electrical conductivity [163], good charge density and low cost [162], the structural destruction (swelling/shrinking) of such materials during the charging/discharging process can significantly interrupt the cycling stability and rate capability performance of supercapacitors [164]. Therefore, the inclusion of carbon materials, for example, porous carbon [165–167], graphene [168–173], graphene oxide [20,174–180], carbon nanotubes [84,181–184] and CNFs [185], has been proposed as a good way to maintain the electrochemical stability of CPs.



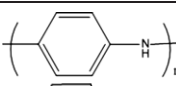
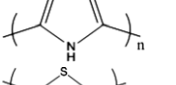
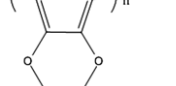
**Table 2**  
Comparison of the electrochemical performances of TMO-based fibres for supercapacitor applications.

Composite electrode	Technique	Electrolyte	Capacitance	Specific energy	Stability performance (%)	Reference
RuO <sub>2</sub> -based fibres						
RuO <sub>x</sub> /GNFs	CVD, electrodeposition	0.5 M H <sub>2</sub> SO <sub>4</sub>	53.76 mF/cm <sup>2</sup>	7.0 × 10 <sup>-5</sup> Wh/cm <sup>2</sup>	83 (5000 cycles)	[111]
RuPM-ACNFs	Electrospinning, activation	6 M KOH	188 F/g	24 Wh/kg	75 (3000 cycles)	[112]
CNFs-RuO <sub>2</sub> -PBI	Modified polyol process, incorporation of phosphoric-acid-doped PBI	0.5 M H <sub>2</sub> SO <sub>4</sub>	1060 F/g	-	98 (1500 cycles)	[113]
RuO <sub>2</sub> /ACNFs	Electrospinning, activation	6 M KOH	530 F/g	-	-	[114]
MnO <sub>2</sub> -based fibres						
MnO <sub>n</sub> /CNFs	Pyrolysis of metal-organic framework containing Mn-ZnBTC	6 M KOH	179 F/g	19.7 Wh/kg	98 (5000 cycles)	[121]
MnO <sub>2</sub> @CFP	Electrodeposition, hydrothermal	0.5 M Li <sub>2</sub> SO <sub>4</sub>	281.9 F/g	-	-	[122]
MnO <sub>2</sub> /VCNFs	Electrochemical oxidation of sputtered Mn shell on VCNFs	1 M Na <sub>2</sub> SO <sub>4</sub>	473 F/g	10 Wh/kg	-	[123]
MnO <sub>2</sub> /CFS	Electrodeposition	1 M Na <sub>2</sub> SO <sub>4</sub>	375 F/g	11.0 Wh/kg	99.2 (5000 cycles)	[124]
C/MnO <sub>x</sub>	Core-shell electrospinning	6 M KOH	213.7 F/g	30 mWh/g	97 (1000 cycles)	[125]
MnO <sub>2</sub> /PCNFs	Electrospinning, in-situ deposition	6 M KOH	520 F/g	-	92.3 (4000 cycles)	[126]
Hollow MnO <sub>2</sub> NFs (eCNFs) (PPBMn)	Hydrothermal	1 M Na <sub>2</sub> SO <sub>4</sub>	291 F/g	-	90.9 (5000 cycles)	[127]
Boron doped-MnO <sub>2</sub>	Electrospinning, carbonisation	6 M KOH	208 F/g	25.66 Wh/kg	90 (3000 cycles)	[128]
	Redox reaction between KMnO <sub>4</sub> and CNFs in the presence of boric acid	0.5 M Na <sub>2</sub> SO <sub>4</sub>	364.8 F/g	-	80.4 (900 cycles)	[129]
MnO <sub>2</sub> /HPCNFs/G	Electrospinning, thermal process	6 M KOH	210 F/g	24 Wh/kg	95.7 (1000 cycles)	[130]
MnO <sub>2</sub> /CNFox//AC ASCs	Catalytic chemical vapour deposition, chemical precipitation	0.5 M K <sub>2</sub> SO <sub>4</sub>	150 F/g	24.8 Wh/kg	92.4 (5000 cycles)	[131]
δ-MnO <sub>2</sub> /SWCNT	Vacuum filtration	PVA-2 M KOH	964 mF/cm <sup>2</sup>	31.8 μW/cm <sup>2</sup>	91 (2000 cycles)	[132]
ZnO@MnO <sub>2</sub> NFs	Colloid pre-treatment, electrodeposition	1 M Na <sub>2</sub> SO <sub>4</sub>	907 F/g	17 Wh/kg	94 (5000 cycles)	[133]
Fe <sub>3</sub> O <sub>4</sub> @CNF <sub>Mn</sub>	Electrospinning, carbonisation	Na <sub>2</sub> SO <sub>4</sub> /PVA	306 F/g	13 Wh/kg	85 (2000 cycles)	[134]
NiO-based fibres						
CNFs/MW (3D) NiO nanowalls	Hydrothermal, CVD	PVA-KOH	12.5 mF/cm <sup>2</sup>	1.74 μW/cm <sup>2</sup>	91 (3000 cycles)	[143]
NiO/CNFs	Direct pyrolysis of metal-organic framework containing Ni and Zn	6 M KOH	234 F/g	33.4 Wh/kg	90 (5000 cycles)	[135]
NiO/CA NFs	Electrospinning with CA	6 M KOH	336 F/g	-	87 (1000 cycles)	[136]
NiO-NFs	Hydrothermal, calcination	1 M KOH	884 F/g	-	87 (1000 cycles)	[145]
NiO-NFs/Ni	Electrospinning, thermal annealing	2 M KOH	737 F/g	22.7 Wh/kg	-	[146]
NiO/PCNFs	Electrospinning, controlled heat treatment	6 M KOH	850 F/g	-	96.7 (10,000 cycles)	[147]
Co <sub>3</sub> O <sub>4</sub> -based fibres						
CNFs-Co	Electrospinning, carbonisation	1 M H <sub>2</sub> SO <sub>4</sub>	911 F/g	-	78 (1000 cycles)	[151]
CoMnO <sub>2</sub> /VGCNFs	Thermal decomposition, annealing	1 M KOH	630 F/g	-	95 (10,000 cycles)	[152]
1D spinel CoMn <sub>2</sub> O <sub>4</sub> (CMO)	Electrospinning	PVA- 1 M H <sub>2</sub> SO <sub>4</sub>	320 F/g	75 Wh/kg	94 (10,000 cycles)	[153]
V <sub>2</sub> O <sub>5</sub> -based fibres						
GO/V <sub>2</sub> O <sub>5</sub> NFs	Electrospinning	2 M KOH	453.8 F/g	-	-	[156]
V <sub>2</sub> O <sub>5</sub> /CNFCs	Electrospinning, carbonisation	6 M KOH	150 F/g	18.8 Wh/kg	82 (100 cycles)	[157]
VMCNFs	Electrospinning, carbonisation	4 M KOH	739 F/g	-	80.3 (1500 cycles)	[158]
Cu <sub>x</sub> O-V <sub>2</sub> O <sub>5</sub> /CNFs	Electrospinning, carbonisation, in-situ deposition	4 M KOH	867.2 F/g	-	92.2 (2000 cycles)	[160]

### 5.1. Polyaniline-based fibres

PANi is one of the best candidates among electrically CPs and has gained much attention due to its outstanding electrochemical properties convincingly good conductivity and a high theoretical capacity [190] with various redox states (leucoemeraldine, emeraldine and perningraniline) [191]. Electrodeposition of the aniline monomer is a

**Table 3**  
Conductivities and chemical structures of PANi, PPy and PEDOT.

Polymer	Chemical structure	Conductivity (S/cm)	Reference
PANi		0.1–5.0	[186,187]
PPy		10–50	[188]
PEDOT		300–500	[189]

common and simple route to produce conducting PANi using a low-pH medium, such as sulphuric acid (H<sub>2</sub>SO<sub>4</sub>), hydrochloric acid (HCl), phosphoric acid (H<sub>3</sub>PO<sub>4</sub>), perchloric acid (HClO<sub>4</sub>) or trifluoroacetic acid (CF<sub>3</sub>COOH) [192].

The supercapacitor performance of PANi can be improved by incorporating carbon nanomaterials for high-performance energy storage. Ke et al. [193] fabricated polyaniline/aminated triazine functionalised carbon nanofibres (PANI/ATFCNFs) by pulsed-current electrochemical polymerisation of aniline, which presented a specific capacitance of 456.73 F/g at a current density of 1.0 A/g and a very low interfacial charge resistance (0.72 Ω). Most importantly, the presence of amino groups on the surface of the ATFCFs is beneficial for controlling the growth of PANi, which manifested a remarkable cycling stability of 84.19% after 1500 successive cycles. Zhou et al. [174] found that PANi nanofibres grew between GO sheets via adsorption of the aniline monomer which can act as a bridge to hinder the stacking of GO layers. The symmetric supercapacitor displayed a high specific energy (30 Wh/kg), which is superior to those of many reported PANi/GO electrodes [194–196], and a superior cycling performance (91.21% after 1000 cycles). This could be a result of the unique architecture of the PANi/GO nanofibres, which facilitates the penetration of electrolyte ions into the electrode.

A novel hybrid containing polyaniline nanofibres and functionalised reduced graphene oxide (PANi NFs/FrGO) was also prepared in several steps including filtration of the GO hybrid suspension and in-situ polymerisation of the aniline monomer, followed by hydrothermal reduction of GO and sulphur-functionalised rGO [197]. Interestingly, the surface area and active sites of the modified PANi NFs/FrGO materials were significantly enhanced after functionalisation with sulphur, showing a high specific capacitance of 324.4 F/g when charged up to 1.2 V and an exceptional specific energy of 16.3 Wh/kg. Moreover, the coulombic efficiency was retained about 92.9% throughout the whole period, which further demonstrates that only little energy is wasted during the charge/discharge process. Yang et al. [198] designed a solid-state fibre-shaped supercapacitor derived from polymerised PANi nanopillars on hierarchical 3D interconnected porous N-doped carbon nanofibre scrolls (PANi-HCNFs) in which PVA/H<sub>3</sub>PO<sub>4</sub> was used as a gel polymer electrolyte. The many omnidirectional pores within the PANi-HCNFs material can provide a better diffusion of ions, which results in an improved specific capacitance (of 339.3 F/g) with a capacitance decay of approximately 25.8% after 3000 cycles. Additionally, a good distribution of PANi nanopillars (with thicknesses ranging between 30 and 50 nm) on the HCNFs surface provides large effective contact area for fast diffusion of active electrolyte ions, resulting to the reduce of charge transfer resistance (3.1 Ω) compared to that of HCNFs alone (8.2 Ω). The electrochemical performance of PANi-HCNFs also remain unchanged under various bending angles (45°, 90°, 135° and 180°), representing its excellent mechanical flexibility.

Mao et al. [53] successfully manufactured a PANi nanowire array/carbon nanofibre/carbon fibre yarn (CFy@CNFs@PANi NWA) by combining electrospinning, carbonisation and subsequent in-situ polymerisation for high-performance yarn-shaped supercapacitors (YSCs). The as-fabricated electrodes exhibited a high areal capacitance of 234 mF/cm<sup>2</sup> at a current density 0.1 mA/cm<sup>2</sup> using 0.02 M aniline monomer (CFy@CNFs@0.02 M PANi NWA). However, the aggregation of PANi NWAs may occur as the concentration increases, which can limit the

kinetics of electron transport and ion diffusion. Interestingly, the device can successfully light up 36 red LEDs connected in series, revealing its potential practical application for flexible electronic devices. Luo et al. [199] developed as-grown carbon nanofibres–helical carbon nanotubes (CNF–HCNT) by catalytic chemical vapour deposition (CCVD), followed by PANi deposition, forming CNF–HCNT–PANi (Fig. 10). To prevent the self-agglomeration of PANi during the charging/discharging process, the CNF–HCNT material was firstly soaked in nitric acid for 2 h to obtain CNF–HCNT–COOH. The abundance of hydroxyl and carbonyl groups attached on the CNF–HCNT facilitates the formation of uniform and thin PANi layers, thus enlarging the active surface area for the redox reaction. The proposed flexible CNF–HCNT–PANi electrode could deliver a high specific capacitance of 660 F/g (at a current density of 1 A/g) and kept a high capacitance value (retained nearly 90.4%) even after 1000 cycles, showing its attractive prospect for high-performance flexible solid supercapacitors.

## 5.2. Polypyrrole-based fibres

PPy is widely recognised as a promising electroactive material for supercapacitors owing to its excellent features, such as a high theoretical capacitance of 620 F/g [162], an enhanced electrical conductivity [200], a high specific energy and a fast charge-discharge ability [201]. Huang et al. [202] studied the capacitive performance of hybrid polypyrrole nanowire/carbon nanofibres (NPPy/CNFs) at different electrodeposition potentials (0.78–0.90 V) and electrodeposition times (100–800 s) of NPPy. The resulting NPPy/CNF material exhibited a high gravimetric capacitance of up to 148.4 F/g at a current density of 0.128 A/g and a deposition time of 400 s with an applied potential of 0.85 V. However, a further increase of the deposition potential to 0.90 V could promote the formation of a bulbous/cauliflower PPy morphology, which would then limit the ion-diffusion process. Furthermore, the as-prepared NPPy/CNFs was able to perfectly retain its electrochemical performance (85% capacitance retained) after 500 bending cycles, which makes it a

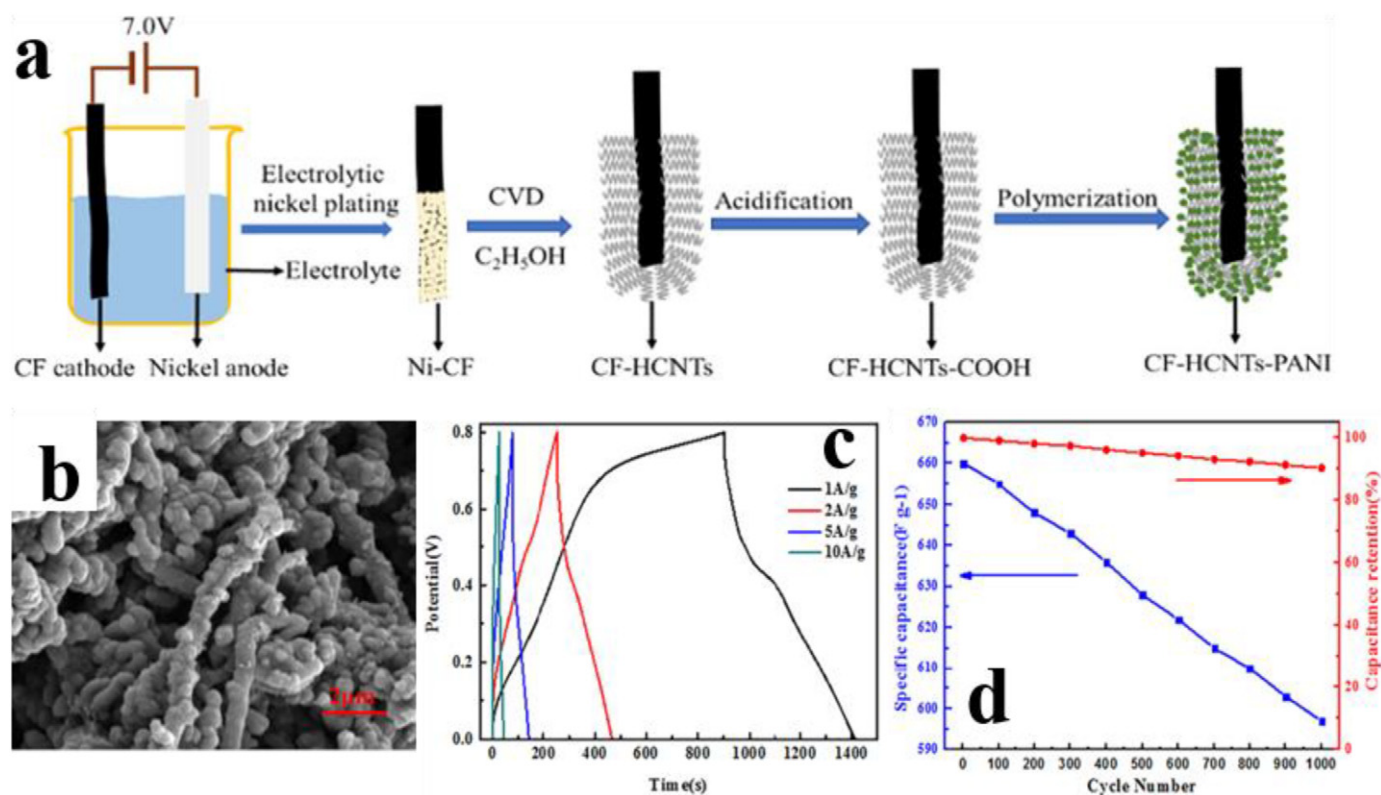


Fig. 10. (a) Schematic illustration for the preparation of flexible CNF–HCNT–PANi electrode. (b) SEM image of CNF–HCNT–PANi with polymerisation time of 4 h. (c) GCD curves of CNF–HCNT–PANi at different current densities (1 to 10 A/g). (d) Stability performance of CNF–HCNT–PANi over 1000 cycles at a current density of 1 A/g [199].

good candidate for flexible and wearable energy storage devices. The enhancement of specific capacitance and rate capability from NPPy/CNFs is attributed from the uniform deposition of the three-dimensional porous structure of NPPy on CNFs surface, which offers large inter-accessible surface area between active sites and electrolyte as well as reducing ion/electron diffusion pathways.

Loose and porous CNT/PPy fibres were synthesised by Guo et al. [203] through several diamond wire-drawing dies approach (Fig. 11). The CNT/PPy fibres exhibited a specific capacitance of 302 F/g with retained rectangular CV shapes, even at a scan rate of 200 mV/s. The outstanding performance of the CNT/PPy fibres can be attributed to the network structure of CNT, which offers a channel for the coated PPy, enabling an efficient electron and ion transportation. In addition, a negligible capacitance degradation of the CNT/PPy fibres was observed after 1000 bending times, which further confirmed their excellent flexibility properties. Chang et al. [204] reported a flexible supercapacitor synthesised from electrochemically deposited PPy on CNFs embedded in a melamine sponge (MS) (PPy-CNFs/MS/PPy-CNFs). The as-prepared PPy-CNFs/MS/PPy-CNF displayed an excellent electrochemical performance with good durability (93% after 20,000 cycles) and a maximum potential window of 3.0 V after five internal tandem ECs were connected in series. Moreover, the remarkable mechanical flexibility of the PPy-CNFs/MS/PPy-CNFs was proven by the unchanged CV profiles of the bent, twisted and compressed states, indicating good electrochemical sustainability even under deformed conditions.

Hamra et al. [205] explored the stability of fabricated polypyrrole-reduced graphene oxide-modified carbon bundle fibres (PPy-rGO) for different charging/discharging cycle numbers (0, 500 and 100 cycles). The full-cell device was assembled by dipping both PPy-rGO electrodes in a polyvinyl alcohol-potassium acetate (PVA-CH<sub>3</sub>COOK) solid-state electrolyte and sandwiching them together. The as-prepared electrode demonstrated a high specific capacitance of 125.99 F/g at the 0th cycle

as compared to 500th cycle (95.22 F/g) and 1000th cycle (49.35 F/g), probably due to a decrease in the pore size with increasing cycle number. More importantly, the cycling deterioration (drained ~60%) of the PPy-rGO composite after consecutive charging/discharging processes could be explained by the mechanical degradation of the polymer chain, which results in a poor diffusion of the electrolyte ions into the electrode. Thus, advanced exploration of hybrid PPy-nanostructured materials is pivotal and urgently needed.

### 5.3. Poly(3,4 ethylenedioxythiophene)-based fibres

PEDOT is one of the members of the polythiophene family which has emerged as a great potential candidate for pseudocapacitor electrodes due to its rapid electrochemical kinetics and excellent intrinsic conductivity [206] compared to other CPs [207]. The preparation of PEDOT can be simply achieved either chemically or by electropolymerisation. Rajesh et al. [208] demonstrated the in-situ polymerisation of PEDOT on a flexible 3D carbon fibre cloth (CFC) through the hydrothermal approach (Fig. 12). In this study, CFC was chosen as a substrate due to its larger accessible surface area, good conductivity, high porosity, chemical stability, flexibility, light weight and cost-effectiveness. A uniform distribution of the growing PEDOT on the CFC surface can be very beneficial for increasing the electrode-electrolyte contact areas and improving the ion diffusion, which can deliver a high specific capacitance of 203 F/g (5 mV/s) and lead to low  $R_{ct}$  (0.2  $\Omega$ ) and  $R_s$  (0.6  $\Omega$ ) values compared to bare CFC. The galvanostatic charge/discharge curves have almost perfect triangular shapes with a small voltage drop ( $IR$  drop) at the beginning of discharging curve, indicating small internal resistance with good electrochemical reversibility. The capacitance of PEDOT/CFC also remained intact (about ~86% after 12,000 cycles), showing the good electrochemical stability of the material. A ternary solid-state supercapacitor composed of carbon black/carbon nanotube/MnO<sub>2</sub>/

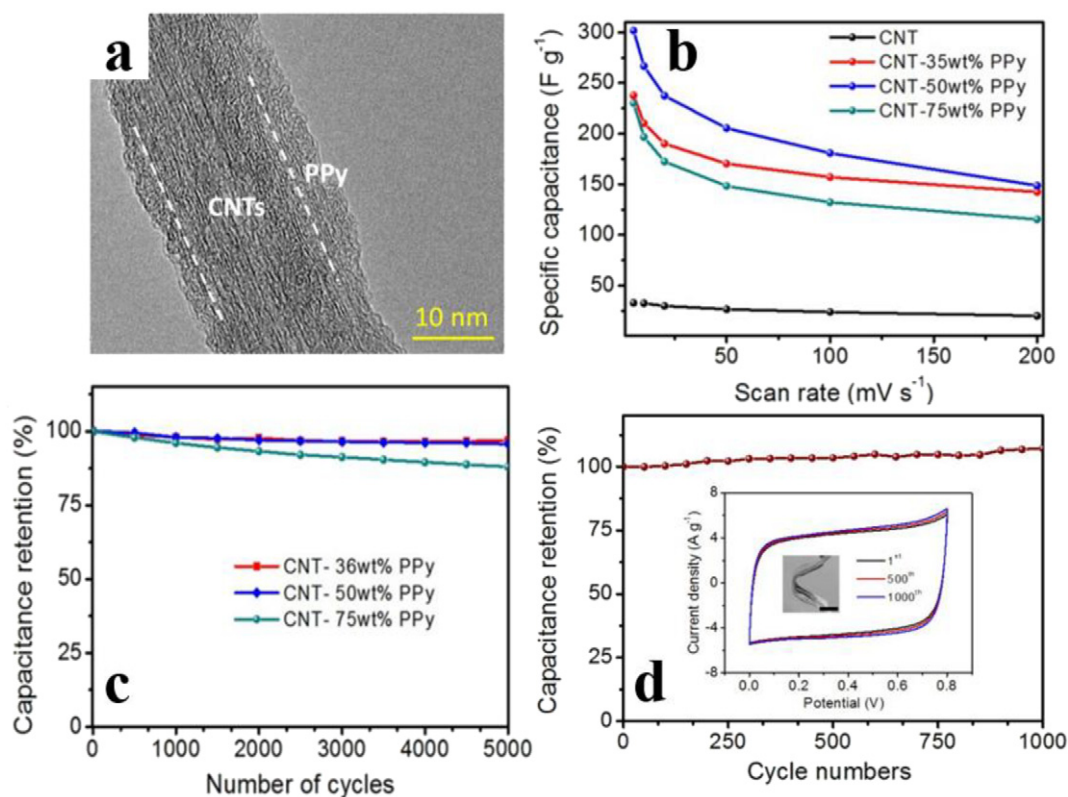
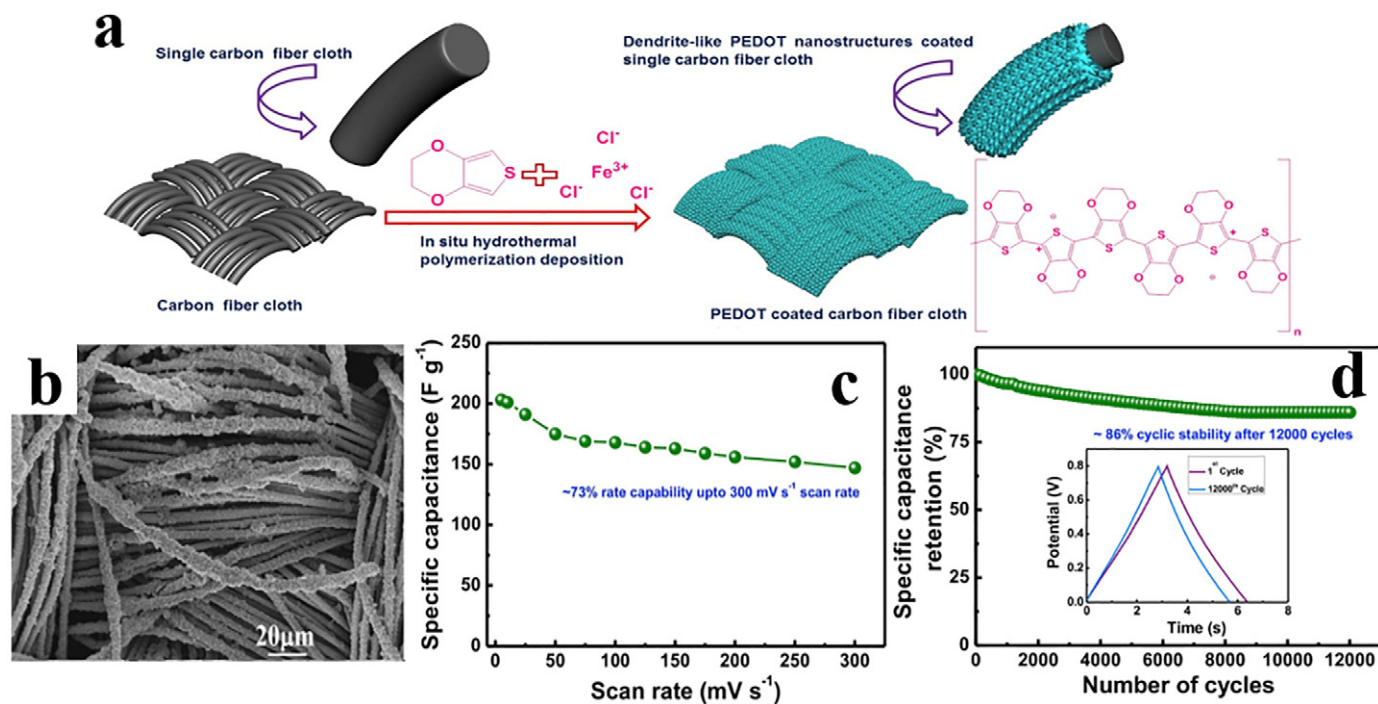


Fig. 11. (a) TEM image of CNT-PPy composite with polypyrrole content of 50 wt%. (b) Specific capacitances against scan rates and (c) cycling stability of different electrodes. (d) Stability performance of flexible fibre-shaped supercapacitor based on CNT-PPy fibres under 90° bending [203].





**Fig. 12.** (a) Schematic illustration of the fabrication of PEDOT/CFC via in-situ hydrothermal polymerisation. (b) A high magnification SEM image of hydrothermally polymerised PEDOT nanostructures coated on CFC. (c) The specific capacitance of symmetrical PEDOT/CFC at different scan rates. (d) Long-term stability of symmetrical PEDOT/CFC over 12,000 cycles at current density 10 A/g [208].

poly(3,4-ethylenedioxythiophene)-poly(styrenesulfonate) was successfully fabricated by Garcia-Torres and Crean [209]. Initially, carbon black (CB)/CNT (CB/CNT) fibres were prepared by wet spinning, followed by modification of the fibres through chemical reduction of potassium permanganate (KMnO<sub>4</sub>). The obtained CB/CNT/MnO<sub>2</sub> fibres were then dip-coated with 0.1 wt% of PEDOT:PSS solution to produce CB/CNT/MnO<sub>2</sub>/PEDOT:PSS. Interestingly, the reported composite exhibited a high specific capacitance of 351 F/g in a three-electrodes system, which may be attributed to the synergistic contribution of each material in the composite. Electropolymerisation is considered a preferable method by which PEDOT is directly grown on the current collector without the addition of binders. Mohd Abdah et al. [20] worked on the fabrication of PEDOT, coated on PVA-GO nanofibres by simple approaches, namely, electrospinning and electropolymerisation. Field-emission scanning electron microscopy images indicated that the web-structure of the PVA-GO nanofibres was fully covered by the porous cauliflower-like structure of PEDOT, which can enlarge the electroactive surface area and enhance the charge storage capacity of the composite. Notably, electrochemical tests revealed that the hybrid PVA-GO/PEDOT material possessed a specific capacitance of 224.27 F/g and specific energy of 9.58 Wh/kg; the capacitance decreased by about 28.9% over 5000 cycles. The poor cycling stability of symmetrical PVA-GO/PEDOT could be possibly due to the swelling and shrinkage of PEDOT structure and subsequent deterioration of the active electrode material. A similar approach was employed by Syed Zainol Abidin et al. [22] to fabricate a PVA-graphene quantum dot (GQD)/PEDOT (PVA-GQD/PEDOT) composite. A uniform PEDOT coating on the PVA-GQD nanofibres proved that the inclusion of GQDs helps to provide more nucleation sites for homogeneous PEDOT deposition. The as-prepared fibre composite exhibited a high specific capacitance (291.86 F/g) at a scan rate of 100 mV/s and a good cycling stability with a capacitance retention of 98% after 1000 cycles. However, the use of PVA-GQD/PEDOT is still limited by its low specific energy (16.95 Wh/kg). The introduction of TMOs and CPs into the nanofibre composites would be a way to address this issue, thereby improving the capacitive properties of the electrodes.

## 6. Transition metal oxide/conducting polymer-based fibres

The pseudocapacitive characteristics of fibre composites can be enhanced by using a combination of TMOs and CPs (TMO/CP-based fibres). Due to their fast/reversible redox reactions and high specific energies, both TMOs and CPs can synergistically offer superior electrochemical performance of the fibre composites by contributing a higher specific capacitance as well as a better electrical conductivity compared to single TMO- and CP-based fibres. Mohd Abdah et al. [83] employed poly(vinyl alcohol)-graphene oxide-manganese oxide (PVA-GO-MnO<sub>2</sub>) microfibrils as a template for PEDOT deposition. The homogeneous distribution of PEDOT on the PVA-GO-MnO<sub>2</sub> microfibrils showed a noticeably higher specific capacitance (144.6 F/g), as compared with PVA-MnO<sub>2</sub>/PEDOT (107.22 F/g), due to the enlarged surface area provided by GO, which also prevents the aggregation of MnO<sub>2</sub> NPs. The potential window of the PVA-GO-MnO<sub>2</sub>/PEDOT microcomposite can be extended to 1.8 V, achieving acceptable cycling stability (91.18% capacitance retained after 1000 cycles). A similar approach (electrospinning and electropolymerisation) has been utilised to prepare a poly(vinyl alcohol)-graphene quantum dot-cobalt oxide/poly(3,4-ethylenedioxythiophene) (PVA-GQD-Co<sub>3</sub>O<sub>4</sub>/PEDOT) material [21]. It was found that the average diameter of the fibres decreased (44 ± 13 nm) after the inclusion of Co<sub>3</sub>O<sub>4</sub> NPs, which shortened the electron transfer pathway while providing more active sites for charge storage. The fibre composite possessed a strikingly high specific capacitance of 361.97 F/g at a scan rate of 100 mV/s. Surprisingly, the rectangular CV curves can be preserved, without discerning any redox peaks, which demonstrates the good electrochemical rate capability of the material. Besides that, the utilisation of CNFs as a conductive substrate is another strategy for improving the performance of TMO/CP-based fibres; for example, a pyrrole (Py) monomer was chemically polymerised on the surface of CNF-MnO<sub>2</sub> to form CNF-MnO<sub>2</sub>/PPy; this symmetric electrode was then assembled with a separator soaked in 1 M KCl electrolyte. The obtained supercapacitor displayed an excellent

electrochemical performance including a high specific capacitance (315.80 F/g) and a remarkable specific energy (13.68 Wh/kg). These promising results could be ascribed to the significant contributions of each material, where the CNFs exhibited excellent mechanical durability and MnO<sub>2</sub> and PPy demonstrated a high theoretical capacity and an appreciable electronic conductivity, respectively [19]. Gong et al. [210] reported the synthesis of porous iron oxide-hydroxide/polypyrrole ( $\gamma$ -FeOOH/PPy) deposited on carbon nanofibres ( $\gamma$ -FeOOH/PPy@CNFs) (anode) and MnO<sub>2</sub>@CNFs (cathode) (denoted as  $\gamma$ -FeOOH/PPy@CNFs//MnO<sub>2</sub>@CNFs) for ASCs. Using a PVA/LiCl gel electrolyte, the rate capability of the assembled device was retained (about 63.8%) as the current density increased from 5 to 100 mA/cm<sup>2</sup> while keeping good cycling stability of 82% after 5000 cycles. This is mainly due to the unique porous morphology of the as-prepared ASCs, which provides numerous electroactive sites and enables effective access of electrolyte ions into the electrodes. Moreover, the CV curves of  $\gamma$ -FeOOH/PPy@CNFs//MnO<sub>2</sub>@CNFs can maintain their original shapes at different bending angles (from 0° to 180°), with a maximum potential window of 1.6 V, due to the outstanding structural flexibility and good electrochemical features of the material. Modification of the CNFs by electrochemical functionalisation, which leads to the presence of abundant hydrophilic groups (i.e. carboxyl, hydroxyl and epoxy functional groups) on the surface, can potentially promote efficient ion-diffusion pathways and enhance the surface wettability of the prepared electrodes. The incorporation of *f*-CNFs with PPy and MnO<sub>2</sub> through in-situ polymerisation and electrodeposition, respectively, led to a superior specific energy (of 42.53 Wh/kg) with a reasonably high specific capacitance (of 409.88 F/g). Moreover, the capacitance of a ternary *f*-CNFs/PPy/MnO<sub>2</sub> composite only decayed by approximately 13.70% after 3000 CV cycles, indicating the good electrochemical stability of the material [18]. A summary of CP- and TMO/CP-based fibre composites with respect to their electrochemical performances for supercapacitors is presented in Table 4.

## 7. Conclusions and outlook

To meet the requirement of sustainable and renewable energy storage for a variety of applications, such as electronic devices, hybrid electrical vehicles as well in large industrial machinery, supercapacitors have been acknowledged as ideal storage devices in fulfilling future demands. The development of nanostructured electrode materials, such as NFs, has gained considerable attention in supercapacitor applications because it has been proven to greatly improve the ion/electron transport through their enlarged SSA, thus increasing the specific capacitance. However, the design and optimum conditions for preparing fibres with superior features still remain a great challenge, and therefore, some factors including the morphology, pore size and surface area of the fibres should be taken into consideration. In this review, recent progress in TMO-, CP- and TMO/CP-based fibres have been pointed out and reviewed. Although TMO- and CP-based fibres can deliver a good electrochemical performance, these individual pseudocapacitor materials still suffer from some limitations including the poor conductivity of TMO, which contributes to a low specific capacitance and causes the structural destruction of the TMO and CP materials during the doping-doping process, thus leading to an inferior stability performance. However, substantial advancements in fibre-based supercapacitors through the incorporation of EDLCs of CNFs with pseudocapacitive materials (TMO or CP) can be employed to overcome the above drawbacks. As for TMO-based fibres, different types of TMO nanoarchitectures (nanoribbons, nanosheets, nanowires, nanoflakes and NPs) should be taken into account to obtain a high pseudocapacitance and a good rate performance of the fibre composites. Moreover, the CP polymerisation routes before incorporation into the fibres (i.e. electrodeposition, in-situ polymerisation, hydrothermal synthesis, CCVD and dip coating) are also important as they can amplify the contact area with the electrolyte, improving the supercapacitive performance of the electrodes. Although the ideal synthesis of TMO/CP-based fibres is believed to overcome the disadvantages of each component, further improvements in the supercapacitive performances of the materials, that is, specific

**Table 4**  
Comparison of the electrochemical performances of CP- and TMO/CP-based fibre composites.

Composite electrode	Technique	Electrolyte	Capacitance	Specific energy	Stability performance (%)	Reference
<b>PANI-based fibres</b>						
PANI/ATFCNFs	Pulse current electrochemical polymerisation	1 M H <sub>2</sub> SO <sub>4</sub>	456 F/g	–	84.2 (1500 cycles)	[193]
PANI/GO NFs	Adsorption of aniline, in-situ polymerisation	1 M H <sub>2</sub> SO <sub>4</sub>	780 F/g	30 Wh/kg	91.2 (1000 cycles)	[174]
PANI NFs/FrGO	Filtration, in-situ polymerisation, hydrothermal reduction, sulphur functionalisation	PVA-H <sub>2</sub> SO <sub>4</sub>	324.4 F/g	16.3 Wh/kg	–	[197]
PANI-HCNFs	Electrospinning, sacrificial template method	PVA-H <sub>3</sub> PO <sub>4</sub>	339.3 F/g	11.6 Wh/kg	74.2 (3000 cycles)	[198]
CFY@CNFs@PANI NWA	Electrospinning, carbonisation, in-situ polymerisation	PVA-H <sub>2</sub> SO <sub>4</sub>	234 mF/cm <sup>2</sup>	21.4 $\mu$ Wh/cm <sup>2</sup>	90 (8000 cycles)	[53]
CNFs-HCNTs-PANI	Catalytic chemical vapour deposition (CCVD)	1 M H <sub>2</sub> SO <sub>4</sub>	660 F/g	–	90.4 (1000 cycles)	[199]
<b>PPy-based fibres</b>						
NPPy/CNFs	Electrodeposition	PVA-H <sub>3</sub> PO <sub>4</sub>	148.4 F/g	–	91 (5000 cycles)	[202]
CNT/PPy fibres	Diamond wire-drawing dies	1 M H <sub>2</sub> SO <sub>4</sub>	302 F/g	3.6 Wh/kg	101 (5000 cycles)	[203]
PPy-CNFs/MS/PPy-CNFs	Electrodeposition	PVA-H <sub>3</sub> PO <sub>4</sub>	189.9 F/g	1.75 mW/cm <sup>3</sup>	93 (20,000 cycles)	[204]
PPy-rGO/modified carbon bundle fibre	Electrodeposition	PVA-CH <sub>3</sub> COOK	125.99 F/g	–	40 (1000 cycles)	[205]
<b>PEDOT-based fibres</b>						
PEDOT/CFC	In-situ polymerisation, hydrothermal	1 M H <sub>2</sub> SO <sub>4</sub>	203 F/g	4.4 Wh/kg	86 (12,000 cycles)	[208]
CB/CNT/MnO <sub>2</sub> /PEDOT:PSS	Wet spinning, chemical reduction, dip coating	0.01 M PBS and 0.1–0.5 M KCl	351 F/g	–	84.2 (1000 cycles)	[209]
PVA-GO/PEDOT	Electrospinning, electrodeposition	1 M KCl	224.3 F/g	10.11 Wh/kg	71.1 (5000 cycles)	[20]
PVA-GQD/PEDOT	Electrospinning, electrodeposition	1 M H <sub>2</sub> SO <sub>4</sub>	291.9 F/g	16.95 Wh/kg	98 (1000 cycles)	[22]
<b>TMO/CP-based fibres</b>						
PVA-GO-MnO <sub>2</sub> /PEDOT	Electrospinning, electrodeposition	1 M KCl	144.6 F/g	9.60 Wh/kg	91.2 (1000 cycles)	[83]
PVA-GQD-Co <sub>3</sub> O <sub>4</sub> /PEDOT	Electrospinning, electrodeposition	1 M H <sub>2</sub> SO <sub>4</sub>	362 F/g	19.98 Wh/kg	96 (1000 cycles)	[21]
CNFs-MnO <sub>2</sub> /PPy	Electrospinning, carbonisation, in-situ polymerisation	1 M KCl	315.80 F/g	13.68 Wh/kg	82.5 (2000 cycles)	[19]
FeOOH/PPy@CNFs//MnO <sub>2</sub> @CNFs	Surface coating, electrodeposition	PVA/LiCl	5.5 F/cm <sup>3</sup>	2 mWh/cm <sup>3</sup>	82 (5000 cycles)	[210]
<i>f</i> -CNFs/PPy/MnO <sub>2</sub>	Electrospinning, carbonisation, electrochemical functionalisation, in-situ polymerisation, electrodeposition	1 M KCl	409.88 F/g	42.53 Wh/kg	86.3 (3000 cycles)	[18]

capacitance, specific energy and long-term stability, are needed for scalable and flexible energy storage devices. It is highly recommended to fabricate fibre-shaped asymmetric supercapacitors (FASCs) by combining two electrode materials with different potential windows. This hybrid electrode design could broaden the potential window, thus exhibiting high specific energy. Furthermore, the introduction of other carbon-based materials [GO, rGO, N-doped graphene, multi-walled carbon nanotubes (MWCNT), PCNFs and nanocrystalline cellulose (NCC)] in the TMO/CP-based fibres can be an alternative approach to achieve an excellent cycling stability for supercapacitors application. In short, tremendous efforts in advancing TMO/CP-based fibres should be made to enlarge the scopes of supercapacitors into flexible, stretchable and compressible devices.

### CRedit authorship contribution statement

**Muhammad Amirul Aizat Mohd Abdah:** Writing - original draft, Data curation. **Nur Hawa Nabilah Azman:** Writing - review & editing. **Shalini Kulandaivalu:** Writing - review & editing. **Yusran Sulaiman:** Supervision.

### Acknowledgement

This work was supported by Universiti Putra Malaysia Research Grant (GP- IPS/2018/9619300).

### References

- [1] M. Rajkumar, C.-T. Hsu, T.-H. Wu, M.-G. Chen, C.-C. Hu, Advanced materials for aqueous supercapacitors in the asymmetric design, *Progress in Natural Science: Materials International* 25 (6) (2015) 527–544.
- [2] W. Wu, L. Yang, S. Chen, Y. Shao, L. Jing, G. Zhao, H. Wei, Core-shell nanospherical polypyrrole/graphene oxide composites for high performance supercapacitors, *RSC Adv.* 5 (111) (2015) 91645–91653.
- [3] W. Du, Y.-L. Bai, J. Xu, H. Zhao, L. Zhang, X. Li, J. Zhang, Advanced metal-organic frameworks (MOFs) and their derived electrode materials for supercapacitors, *J. Power Sources* 402 (2018) 281–295.
- [4] B.Y. Guan, A. Kushima, L. Yu, S. Li, J. Li, X.W. Lou, Coordination polymers derived general synthesis of multishelled mixed metal-oxide particles for hybrid supercapacitors, *Adv. Mater.* 29 (17) (2017), 1605902.
- [5] J. Liu, J. Jiang, C. Cheng, H. Li, J. Zhang, H. Gong, H.J. Fan,  $\text{Co}_3\text{O}_4$  nanowire/ $\text{MnO}_2$  ultrathin nanosheet core/shell arrays: a new class of high-performance pseudocapacitive materials, *Adv. Mater.* 23 (18) (2011) 2076–2081.
- [6] H.-J. Qiu, L. Liu, Y.-P. Mu, H.-J. Zhang, Y. Wang, Designed synthesis of cobalt-oxide-based nanomaterials for superior electrochemical energy storage devices, *Nano Res.* 8 (2) (2015) 321–339.
- [7] N. Agnihotri, P. Sen, A. De, M. Mukherjee, Hierarchically designed PEDOT encapsulated graphene- $\text{MnO}_2$  nanocomposite as supercapacitors, *Mater. Res. Bull.* 88 (2017) 218–225.
- [8] M.A.A. Mohd Abdah, N.H.N. Azman, S. Kulandaivalu, Y. Sulaiman, Asymmetric supercapacitor of functionalised electrospun carbon fibers/poly(3,4-ethylenedioxythiophene)/manganese oxide/activated carbon with superior electrochemical performance, *Scientific Reports* 9 (2019) 16782.
- [9] Y. Li, X. Han, T. Yi, Y. He, X. Li, Review and prospect of  $\text{NiCo}_2\text{O}_4$ -based composite materials for supercapacitor electrodes, *Journal of Energy Chemistry* 31 (2018) 54–78.
- [10] A. González, E. Goikolea, J.A. Barrera, R. Mysyk, Review on supercapacitors: technologies and materials, *Renew. Sust. Energ. Rev.* 58 (2016) 1189–1206.
- [11] Q. Li, S. Zheng, Y. Xu, H. Xue, H. Pang, Ruthenium based materials as electrode materials for supercapacitors, *Chem. Eng. J.* 333 (2018) 505–518.
- [12] A. Nirmalesh Naveen, S. Selladurai, Fabrication and performance evaluation of symmetrical supercapacitor based on manganese oxide nanorods-PANI composite, *Mater. Sci. Semicond. Process.* 40 (2015) 468–478.
- [13] S. He, W. Chen, 3D graphene nanomaterials for binder-free supercapacitors: scientific design for enhanced performance, *Nanoscale* 7 (16) (2015) 6957–6990.
- [14] C. Zhao, A. Tan, G. Pastorin, H.K. Ho, Nanomaterial scaffolds for stem cell proliferation and differentiation in tissue engineering, *Biotechnol. Adv.* 31 (5) (2013) 654–668.
- [15] J.V. Patil, S.S. Mali, A.S. Kamble, C.K. Hong, J.H. Kim, P.S. Patil, Electrospinning: a versatile technique for making of 1D growth of nanostructured nanofibres and its applications: An experimental approach, *Appl. Surf. Sci.* 423 (2017) 641–674.
- [16] R. Sridhar, R. Lakshminarayanan, K. Madhaiyan, V.A. Barathi, K.H.C. Limh, S. Ramakrishna, Electrospun nanoparticles and electrospun nanofibres based on natural materials: applications in tissue regeneration, drug delivery and pharmaceuticals, *Chem. Soc. Rev.* 44 (3) (2015) 790–814.
- [17] Q. Liu, J. Zhu, L. Zhang, Y. Qiu, Recent advances in energy materials by electrospinning, *Renew. Sust. Energ. Rev.* 81 (2018) 1825–1858.
- [18] M.A.A. Mohd Abdah, N. Abdul Rahman, Y. Sulaiman, Ternary functionalised carbon nanofibre/polypyrrole/manganese oxide as high specific energy electrode for supercapacitor, *Ceramics International* 45 (7, Part A) (2019) 8433–8439.
- [19] M.A.A. Mohd Abdah, N. Mohammed Moday Aldris Edris, S. Kulandaivalu, N. Abdul Rahman, Y. Sulaiman, Supercapacitor with superior electrochemical properties derived from symmetrical manganese oxide-carbon fibre coated with polypyrrole, *Int. J. Hydrog. Energy* 43 (36) (2018) 17328–17337.
- [20] M.A.A. Mohd Abdah, N.A. Zubair, N.H.N. Azman, Y. Sulaiman, Fabrication of PEDOT coated PVA-GO nanofibre for supercapacitor, *Mater. Chem. Phys.* 192 (2017) 161–169.
- [21] S.N.J. Syed Zainol Abidin, M.S. Mamat, S.A. Rasyid, Z. Zainal, Y. Sulaiman, Electropolymerization of poly(3,4-ethylenedioxythiophene) onto poly(vinyl alcohol)-graphene quantum dot-cobalt oxide nanofibre composite for high-performance supercapacitor, *Electrochim. Acta* 261 (2018) 548–556.
- [22] S.N.J.S.Z. Abidin, S. Mamat, S.A. Rasyid, Z. Zainal, Y. Sulaiman, Fabrication of poly(vinyl alcohol)-graphene quantum dots coated with poly(3,4-ethylenedioxythiophene) for supercapacitor, *J. Polym. Sci. A Polym. Chem.* 56 (1) (2018) 50–58.
- [23] S. Peng, L. Li, J. Kong Yoong Lee, L. Tian, M. Srinivasan, S. Adams, S. Ramakrishna, Electrospun carbon nanofibres and their hybrid composites as advanced materials for energy conversion and storage, *Nano Energy* 22 (2016) 361–395.
- [24] N.A. Zubair, N.A. Rahman, H.N. Lim, Y. Sulaiman, Production of conductive PEDOT-coated PVA-GO composite nanofibres, *Nanoscale Res. Lett.* 12 (1) (2017) 113.
- [25] X. Li, Y. Chen, H. Huang, Y.W. Mai, L. Zhou, Electrospun carbon-based nanostructured electrodes for advanced energy storage - a review, *Energy Storage Materials* 5 (2016) 58–92.
- [26] C. Tran, V. Kalra, Fabrication of porous carbon nanofibres with adjustable pore sizes as electrodes for supercapacitors, *J. Power Sources* 235 (2013) 289–296.
- [27] L. Xu, Rationally designed hierarchical  $\text{NiCo}_2\text{O}_4$ - $\text{C}/\text{Ni}(\text{OH})_2$  core-shell nanofibres for high performance supercapacitors, *Carbon* 152 (2019) 652–660(v.152).
- [28] B. Yan, S. Matsushita, K. Akagi, Aligned carbon and graphite fibres prepared from poly(3,4-ethylenedioxythiophene) single crystals synthesized by solid-state polymerization and their supercapacitor performance, *J. Mater. Chem. C* 5 (15) (2017) 3823–3829.
- [29] S. Tan, T.J. Kraus, K.D. Li-Oakey, Understanding the supercapacitor properties of electrospun carbon nanofibres from powder river basin coal, *Fuel* 245 (2019) 148–159.
- [30] Q.-Z. Zhang, D. Zhang, Z.-C. Miao, X.-L. Zhang, S.-L. Chou, Research progress in  $\text{MnO}_2$ -carbon based supercapacitor electrode materials, *Small* 14 (24) (2018) 1702883.
- [31] S. Xie, S. Liu, F. Cheng, X. Lu, Recent advances toward achieving high-performance carbon-fibre materials for supercapacitors, *ChemElectroChem* 5 (4) (2018) 571–582.
- [32] D. Yu, Q. Qian, L. Wei, W. Jiang, K. Goh, J. Wei, J. Zhang, Y. Chen, Emergence of fibre supercapacitors, *Chem. Soc. Rev.* 44 (3) (2015) 647–662.
- [33] J. Banerjee, K. Dutta, M.A. Kader, S.K. Nayak, An overview on the recent developments in polyaniline-based supercapacitors, *Polym. Adv. Technol.* 30 (8) (2019) 1902–1921.
- [34] Poonam, K. Sharma, A. Arora, S.K. Tripathi, Review of supercapacitors: materials and devices, *Journal of Energy Storage* 21 (2019) 801–825.
- [35] A. Muzaffar, M.B. Ahamed, K. Deshmukh, J. Thirumalai, A review on recent advances in hybrid supercapacitors: design, fabrication and applications, *Renew. Sust. Energ. Rev.* 101 (2019) 123–145.
- [36] R. Dubey, V. Guruviah, Review of carbon-based electrode materials for supercapacitor energy storage, *Ionics* 25 (4) (2019) 1419–1445.
- [37] C.L. Casper, J.S. Stephens, N.G. Tassi, D.B. Chase, J.F. Rabolt, Controlling surface morphology of electrospun polystyrene fibres: effect of humidity and molecular weight in the electrospinning process, *Macromolecules* 37 (2) (2004) 573–578.
- [38] A.L. Yarin, E. Zussman, J.H. Wendorff, A. Greiner, Material encapsulation and transport in core-shell micro/nanofibres, polymer and carbon nanotubes and micro/nanochannels, *J. Mater. Chem.* 17 (25) (2007) 2585–2599.
- [39] J. Zhang, K. Qiu, B. Sun, J. Fang, K. Zhang, H. Ei-Hamshary, S.S. Al-Deyab, X. Mo, The aligned core-sheath nanofibres with electrical conductivity for neural tissue engineering, *J. Mater. Chem. B* 2 (45) (2014) 7945–7954.
- [40] C. Ma, Z. Li, J. Li, Q. Fan, L. Wu, J. Shi, Y. Song, Lignin-based hierarchical porous carbon nanofibre films with superior performance in supercapacitors, *Appl. Surf. Sci.* 456 (2018) 568–576.
- [41] Y. Zhao, W. Kang, L. Li, G. Yan, X. Wang, X. Zhuang, B. Cheng, Solution blown silicon carbide porous nanofibre membrane as electrode materials for supercapacitors, *Electrochim. Acta* 207 (2016) 257–265.
- [42] T. Zhou, Q. Jiang, L. Wang, Z. Qiu, Y. Liu, J. Zhou, B. Liu, Facile preparation of nitrogen-enriched hierarchical porous carbon nanofibres by  $\text{Mg}(\text{OAc})_2$ -assisted electrospinning for flexible supercapacitors, *Appl. Surf. Sci.* 456 (2018) 827–834.
- [43] B.-H. Kim, K.S. Yang, H.-G. Woo, K. Oshida, Supercapacitor performance of porous carbon nanofibre composites prepared by electrospinning polymethylhydrosiloxane (PMHS)/polyacrylonitrile (PAN) blend solutions, *Synth. Met.* 161 (13) (2011) 1211–1216.
- [44] L. Zhang, Y. Jiang, L. Wang, C. Zhang, S. Liu, Hierarchical porous carbon nanofibres as binder-free electrode for high-performance supercapacitor, *Electrochim. Acta* 196 (2016) 189–196.
- [45] K. Wei, K.-O. Kim, K.-H. Song, C.-Y. Kang, J.S. Lee, M. Gopiraman, I.-S. Kim, Nitrogen- and oxygen-containing porous ultrafine carbon nanofibre: a highly flexible electrode material for supercapacitor, *Journal of Materials Science & Technology* 33 (5) (2017) 424–431.
- [46] L. Chen, D. Li, L. Chen, P. Si, J. Feng, L. Zhang, Y. Li, J. Lou, L. Ci, Core-shell structured carbon nanofibres yarn@polypyrrole@graphene for high performance all-solid-state fibre supercapacitors, *Carbon* 138 (2018) 264–270.



- [47] W. Wang, Y. Yuan, J. Yang, L. Meng, H. Tang, Y. Zeng, Z. Ye, J. Lu, Hierarchical core-shell  $\text{Co}_3\text{O}_4/\text{graphene}$  hybrid fibres: potential electrodes for supercapacitors, *J. Mater. Sci.* 53 (8) (2018) 6116–6123.
- [48] X. Lu, C. Shen, Z. Zhang, E. Barrios, L. Zhai, Core-shell composite fibres for high-performance flexible supercapacitor electrodes, *ACS Appl. Mater. Interfaces* 10 (4) (2018) 4041–4049.
- [49] Q. Xie, R. Bao, C. Xie, A. Zheng, S. Wu, Y. Zhang, R. Zhang, P. Zhao, Core-shell N-doped active carbon fibre@graphene composites for aqueous symmetric supercapacitors with high-energy and high-power density, *J. Power Sources* 317 (2016) 133–142.
- [50] D. Zhang, Y. Zhang, Y. Luo, P.K. Chu, Highly porous honeycomb manganese oxide@carbon fibres core-shell nanocables for flexible supercapacitors, *Nano Energy* 13 (2015) 47–57.
- [51] S. Chen, W. Ma, Y. Cheng, Z. Weng, B. Sun, L. Wang, W. Chen, F. Li, M. Zhu, H.-M. Cheng, Scalable non-liquid-crystal spinning of locally aligned graphene fibres for high-performance wearable supercapacitors, *Nano Energy* 15 (2015) 642–653.
- [52] Z. Lin, Z. Li, K.-s. Moon, Y. Fang, Y. Yao, L. Li, C.-p. Wong, Robust vertically aligned carbon nanotube-carbon fibre paper hybrid as versatile electrodes for supercapacitors and capacitive deionization, *Carbon* 63 (2013) 547–553.
- [53] N. Mao, W. Chen, J. Meng, Y. Li, K. Zhang, X. Qin, H. Zhang, C. Zhang, Y. Qiu, S. Wang, Enhanced electrochemical properties of hierarchically sheath-core aligned carbon nanofibres coated carbon fibre yarn electrode-based supercapacitor via polyaniline nanowire array modification, *J. Power Sources* 399 (2018) 406–413.
- [54] M. Yanilmaz, M. Dirican, A.M. Asiri, X. Zhang, Flexible polyaniline-carbon nanofibre supercapacitor electrodes, *Journal of Energy Storage* 24 (2019), 100766.
- [55] S. Ma, Y. Wang, Z. Liu, M. Huang, H. Yang, Z. Xu, Preparation of carbon nanofibre with multilevel gradient porous structure for supercapacitor and  $\text{CO}_2$  adsorption, *Chem. Eng. Sci.* 205 (2019) 181–189.
- [56] Y. Luan, G. Nie, X. Zhao, N. Qiao, X. Liu, H. Wang, X. Zhang, Y. Chen, Y.-Z. Long, The integration of  $\text{SnO}_2$  dots and porous carbon nanofibres for flexible supercapacitors, *Electrochim. Acta* 308 (2019) 121–130.
- [57] C. Ma, S. Ruan, J. Wang, D. Long, W. Qiao, L. Ling, Free-standing carbon nanofibre fabrics for high performance flexible supercapacitor, *J. Colloid Interface Sci.* 531 (2018) 513–522.
- [58] X. Shi, S. Zheng, Z.-S. Wu, X. Bao, Recent advances of graphene-based materials for high-performance and new-concept supercapacitors, *Journal of Energy Chemistry* 27 (1) (2018) 25–42.
- [59] K. Wu, J. Zhao, X. Zhang, H. Zhou, M. Wu, Hierarchical mesoporous  $\text{MoO}_3$  sphere as highly effective supercapacitor electrode, *J. Taiwan Inst. Chem. Eng.* 102 (2019) 212–217.
- [60] W. Wu, D. Niu, J. Zhu, Y. Gao, D. Wei, C. Zhao, C. Wang, F. Wang, L. Wang, L. Yang, Hierarchical architecture of  $\text{Ti}_3\text{C}_2\text{@PDA}/\text{NiCo}_2\text{S}_4$  composite electrode as high-performance supercapacitors, *Ceram. Int.* 45 (13) (2019) 16261–16269.
- [61] Y.-M. Lian, W. Utetiwabo, Y. Zhou, Z.-H. Huang, L. Zhou, F. Muhammad, R.-J. Chen, W. Yang, From upcycled waste polyethylene plastic to graphene/mesoporous carbon for high-voltage supercapacitors, *J. Colloid Interface Sci.* 557 (2019) 55–64.
- [62] R. Atchudan, T.N.J. Edison, S. Perumal, P. Thirukumar, R. Vinodh, Y.R. Lee, Green synthesis of nitrogen-doped carbon nanograss for supercapacitors, *J. Taiwan Inst. Chem. Eng.* 102 (2019) 475–486.
- [63] W.H. Low, P.S. Khiew, S.S. Lim, C.W. Siong, E.R. Ezeigwe, Recent development of mixed transition metal oxide and graphene/mixed transition metal oxide based hybrid nanostructures for advanced supercapacitors, *J. Alloys Compd.* 775 (2019) 1324–1356.
- [64] S. Kulandaivalu, Y. Sulaiman, Recent advances in layer-by-layer assembled conducting polymer based composites for supercapacitors, *Energies* 12 (11) (2019).
- [65] S.I. Wong, J. Sunarso, B.T. Wong, H. Lin, A. Yu, B. Jia, Towards enhanced energy density of graphene-based supercapacitors: current status, approaches, and future directions, *J. Power Sources* 396 (2018) 182–206.
- [66] Y. Huang, H. Li, Z. Wang, M. Zhu, Z. Pei, Q. Xue, Y. Huang, C. Zhi, Nanostructured polypyrrole as a flexible electrode material of supercapacitor, *Nano Energy* 22 (2016) 422–438.
- [67] A. Afif, S.M.H. Rahman, A. Tasfiah Azad, J. Zaini, M.A. Islan, A.K. Azad, Advanced materials and technologies for hybrid supercapacitors for energy storage – a review, *Journal of Energy Storage* 25 (2019), 100852.
- [68] Y.-J. Peng, T.-H. Wu, C.-T. Hsu, S.-M. Li, M.-G. Chen, C.-C. Hu, Electrochemical characteristics of the reduced graphene oxide/carbon nanotube/polypyrrole composites for aqueous asymmetric supercapacitors, *J. Power Sources* 272 (Supplement C) (2014) 970–978.
- [69] Y. Wu, F. Ran, Vanadium nitride quantum dot/nitrogen-doped microporous carbon nanofibres electrode for high-performance supercapacitors, *J. Power Sources* 344 (Supplement C) (2017) 1–10.
- [70] M. Xianwen, T.A. Hatton, C.R. Gregory, A review of electrospun carbon fibres as electrode materials for energy storage, *Curr. Org. Chem.* 17 (13) (2013) 1390–1401.
- [71] L. Tong, J. Liu, S.M. Boyer, L.A. Sonnenberg, M.T. Fox, D. Ji, J. Feng, W.E. Bernier, W.E. Jones Jr, Vapor-phase polymerized poly(3,4-ethylenedioxythiophene) (PEDOT)/ $\text{TiO}_2$  composite fibres as electrode materials for supercapacitors, *Electrochim. Acta* 224 (2017) 133–141.
- [72] J.K. Gan, Y.S. Lim, A. Pandikumar, N.M. Huang, H.N. Lim, Graphene/polypyrrole-coated carbon nanofibre core-shell architecture electrode for electrochemical capacitors, *RSC Adv.* 5 (17) (2015) 12692–12699.
- [73] W.-M. Chang, C.-C. Wang, C.-Y. Chen, Plasma-induced polyaniline grafted on carbon nanotube-embedded carbon nanofibres for high-performance supercapacitors, *Electrochim. Acta* 212 (2016) 130–140.
- [74] J.K. Gan, Y.S. Lim, N.M. Huang, H.N. Lim, Hybrid silver nanoparticle/nanocluster-decorated polypyrrole for high-performance supercapacitors, *RSC Adv.* 5 (92) (2015) 75442–75450.
- [75] Y. Tian, C. Yang, X. Song, J. Liu, L. Zhao, P. Zhang, L. Gao, Engineering the volumetric effect of Polypyrrole for auto-deformable supercapacitor, *Chem. Eng. J.* 374 (2019) 59–67.
- [76] H. Zhuo, Y. Hu, Z. Chen, L. Zhong, Cellulose carbon aerogel/PPy composites for high-performance supercapacitor, *Carbohydr. Polym.* 215 (2019) 322–329.
- [77] Z. Yang, J. Ma, B. Bai, A. Qiu, D. Lolic, D. Shi, M. Chen, Free-standing PEDOT/polyaniline conductive polymer hydrogel for flexible solid-state supercapacitors, *Electrochim. Acta* 322 (2019), 134769.
- [78] X. Li, M. Zhou, H. Xu, G. Wang, Z. Wang, Synthesis and electrochemical performances of a novel two-dimensional nanocomposite: polyaniline-coated laponite nanosheets, *J. Mater. Sci.* 49 (19) (2014) 6830–6837.
- [79] H. Wang, M. Gao, Y. Zhu, H. Zhou, H. Liu, L. Gao, M. Wu, A flexible 3-D structured carbon molecular sieve@PEDOT composite electrode for supercapacitor, *J. Electroanal. Chem.* 826 (2018) 191–197.
- [80] M. Zhou, F. Pu, Z. Wang, S. Guan, Nitrogen-doped porous carbons through KOH activation with superior performance in supercapacitors, *Carbon* 68 (2014) 185–194.
- [81] R. Ravit, J. Abdullah, I. Ahmad, Y. Sulaiman, Electrochemical performance of poly(3,4-ethylenedioxythiophene)/nanocrystalline cellulose (PEDOT/NCC) film for supercapacitor, *Carbohydr. Polym.* 203 (2019) 128–138.
- [82] N.H.N. Azman, H.N. Lim, Y. Sulaiman, Effect of electropolymerization potential on the preparation of PEDOT/graphene oxide hybrid material for supercapacitor application, *Electrochim. Acta* 188 (2016) 785–792.
- [83] M.A.A. Mohd Abdah, N. Abdul Rahman, Y. Sulaiman, Enhancement of electrochemical performance based on symmetrical poly-(3,4-ethylenedioxythiophene) coated polyvinyl alcohol/graphene oxide/manganese oxide microfiber for supercapacitor, *Electrochim. Acta* 259 (Supplement C) (2018) 466–473.
- [84] M.A.A. Mohd Abdah, N.S. Mohd Razali, P.T. Lim, S. Kulandaivalu, Y. Sulaiman, One-step potentiostatic electrodeposition of polypyrrole/graphene oxide/multi-walled carbon nanotubes ternary nanocomposite for supercapacitor, *Mater. Chem. Phys.* 219 (2018) 120–128.
- [85] Y. Sulaiman, M.K.S. Azmi, M.A.A. Mohd Abdah, N.H.N. Azman, One step electrodeposition of poly-(3,4-ethylenedioxythiophene)/graphene oxide/cobalt oxide ternary nanocomposite for high performance supercapacitor, *Electrochim. Acta* 253 (2017) 581–588.
- [86] B. Zhang, F. Kang, J.-M. Tarascon, J.-K. Kim, Recent advances in electrospun carbon nanofibres and their application in electrochemical energy storage, *Prog. Mater. Sci.* 76 (2016) 319–380.
- [87] M.A.A. Mohd Abdah, N.H.N. Azman, S. Kulandaivalu, A.H. Abdullah, Y. Sulaiman, Potentiostatic deposition of poly(3,4-ethylenedioxythiophene) and manganese oxide on porous functionalised carbon fibers as an advanced electrode for asymmetric supercapacitor, *Journal of Power Sources* 444 (2019) 227324.
- [88] S. Bhoyate, P.K. Kahol, B. Sapkota, S.R. Mishra, F. Perez, R.K. Gupta, Polystyrene activated linear tube carbon nanofibre for durable and high-performance supercapacitors, *Surf. Coat. Technol.* 345 (2018) 113–122.
- [89] C. Ma, R. Wang, Z. Xie, H. Zhang, Z. Li, J. Shi, Preparation and molten salt-assisted KOH activation of porous carbon nanofibres for use as supercapacitor electrodes, *J. Porous. Mater.* 24 (6) (2017) 1437–1445.
- [90] J. Yan, J.-H. Choi, Y.G. Jeong, Freestanding supercapacitor electrode applications of carbon nanofibres based on polyacrylonitrile and polyhedral oligomeric silsesquioxane, *Mater. Des.* 139 (2018) 72–80.
- [91] S.K. Nataraj, K.S. Yang, T.M. Aminabhavi, Polyacrylonitrile-based nanofibres – a state-of-the-art review, *Progress in Polymer Science (Oxford)* 37 (3) (2012) 487–513.
- [92] H. Feng, H. Hu, H. Dong, Y. Xiao, Y. Cai, B. Lei, Y. Liu, M. Zheng, Hierarchical structured carbon derived from bagasse wastes: a simple and efficient synthesis route and its improved electrochemical properties for high-performance supercapacitors, *J. Power Sources* 302 (2016) 164–173.
- [93] L. Qie, W. Chen, H. Xu, X. Xiong, Y. Jiang, F. Zou, X. Hu, Y. Xin, Z. Zhang, Y. Huang, Synthesis of functionalized 3D hierarchical porous carbon for high-performance supercapacitors, *Energy Environ. Sci.* 6 (8) (2013) 2497–2504.
- [94] C.W. Huang, C.T. Hsieh, P.L. Kuo, H. Teng, Electric double layer capacitors based on a composite electrode of activated mesophase pitch and carbon nanotubes, *J. Mater. Chem.* 22 (15) (2012) 7314–7322.
- [95] D. Lee, J.Y. Jung, M.J. Jung, Y.S. Lee, Hierarchical porous carbon fibres prepared using a  $\text{SiO}_2$  template for high-performance EDLCs, *Chem. Eng. J.* 263 (2015) 62–70.
- [96] M.S.A. Rahaman, A.F. Ismail, A. Mustafa, A review of heat treatment on polyacrylonitrile fibre, *Polym. Degrad. Stab.* 92 (8) (2007) 1421–1432.
- [97] D. Zhu, C. Xu, N. Nakura, M. Matsuo, Study of carbon films from PAN/VGCF composites by gelation/crystallization from solution, *Carbon* 40 (3) (2002) 363–373.
- [98] J.H. Zheng, R.M. Zhang, P.F. Yu, X.G. Wang, Binary transition metal oxides (BTMO) (Co-Zn, Co-Cu) synthesis and high supercapacitor performance, *J. Alloys Compd.* 772 (2019) 359–365.
- [99] Z. Zhang, Z. Xu, Z. Yao, Y. Meng, Q. Xia, D. Li, Z. Jiang, Ultrahigh capacitance of  $\text{TiO}_2$  nanotube arrays/C/ $\text{MnO}_2$  electrode for supercapacitor, *J. Alloys Compd.* 805 (2019) 396–403.
- [100] S. Muthkuri, S. Chakrabarti, H. Gupta, B. Padya, T.N. Rao, P.K. Jain, Synthesis of  $\text{MnO}_2$  nano-flakes for high performance supercapacitor application, *Materials Today: Proceedings* (2019).
- [101] T.-F. Yi, J. Mei, B. Guan, P. Cui, S. Luo, Y. Xie, Y. Liu, Construction of spherical  $\text{NiO}/\text{MnO}_2$  with core-shell structure obtained by depositing  $\text{MnO}_2$  nanoparticles on  $\text{NiO}$  nanosheets for high-performance supercapacitor, *Ceram. Int.* 46 (2020) 421–429.
- [102] J. Lin, Y. Yan, H. Wang, X. Zheng, Z. Jiang, Y. Wang, J. Qi, J. Cao, W. Fei, J. Feng, Hierarchical  $\text{Fe}_2\text{O}_3$  and  $\text{NiO}$  nanotube arrays as advanced anode and cathode electrodes for high-performance asymmetric supercapacitors, *J. Alloys Compd.* 794 (2019) 255–260.
- [103] P. Wang, H. Zhou, C. Meng, Z. Wang, K. Akhtar, A. Yuan, Cyanometallic framework-derived hierarchical  $\text{Co}_3\text{O}_4$ - $\text{NiO}$ /graphene foam as high-performance binder-free electrodes for supercapacitors, *Chem. Eng. J.* 369 (2019) 57–63.

- [104] T. Wang, H.C. Chen, F. Yu, X.S. Zhao, H. Wang, Boosting the cycling stability of transition metal compounds-based supercapacitors, *Energy Storage Materials* 16 (2019) 545–573.
- [105] Z. Fan, X. Huang, C. Tan, H. Zhang, Thin metal nanostructures: synthesis, properties and applications, *Chem. Sci.* 6 (1) (2015) 95–111.
- [106] C.-Q. Yi, J.-P. Zou, H.-Z. Yang, X. Leng, Recent advances in pseudocapacitor electrode materials: transition metal oxides and nitrides, *Trans. Nonferrous Metals Soc. China* 28 (10) (2018) 1980–2001.
- [107] C. Tang, Z. Tang, H. Gong, Hierarchically porous Ni-co oxide for high reversibility asymmetric full-cell supercapacitors, *J. Electrochem. Soc.* 159 (5) (2012) A651–A656.
- [108] C.-C. Hu, K.-H. Chang, M.-C. Lin, Y.-T. Wu, Design and tailoring of the nanotubular arrayed architecture of hydrous RuO<sub>2</sub> for next generation supercapacitors, *Nano Lett.* 6 (12) (2006) 2690–2695.
- [109] L.Y. Chen, Y. Hou, J.L. Kang, A. Hirata, T. Fujita, M.W. Chen, Toward the theoretical capacitance of RuO<sub>2</sub> reinforced by highly conductive nanoporous gold, *Adv. Energy Mater.* 3 (7) (2013) 851–856.
- [110] Y. Xu, J. Wei, L. Tan, J. Yu, Y. Chen, A facile approach to NiCo<sub>2</sub>O<sub>4</sub> intimately standing on nitrogen doped graphene sheets by one-step hydrothermal synthesis for supercapacitors, *J. Mater. Chem. A* 3 (13) (2015) 7121–7131.
- [111] J.-J. Jhao, C.-H. Lin, T.-K. Yeh, H.-C. Wu, M.-C. Tsai, C.-K. Hsieh, The coaxial nanostructure of ruthenium oxide thin films coated onto the vertically grown graphitic nanofibres for electrochemical supercapacitor, *Surf. Coat. Technol.* 320 (2017) 263–269.
- [112] B.-H. Kim, C.H. Kim, D.G. Lee, Mesopore-enriched activated carbon nanofibre web containing RuO<sub>2</sub> as electrode material for high-performance supercapacitors, *J. Electroanal. Chem.* 760 (2016) 64–70.
- [113] B.K. Balan, H.D. Chaudhari, U.K. Kharul, S. Kurungot, Carbon nanofibre–RuO<sub>2</sub>–poly (benzimidazole) ternary hybrids for improved supercapacitor performance, *RSC Adv.* 3 (7) (2013) 2428–2436.
- [114] C. Kim, Y.H. Joo, J.H. Kim, W.J. Lee, K.S. Yang, Performances of electrochemical hybrid supercapacitor of RuO<sub>2</sub>/activated carbon nanofibres from electrospinning, *WSEAS Transactions on Systems* 5 (8) (2006) 1971–1975.
- [115] J. Qu, L. Shi, C. He, F. Gao, B. Li, Q. Zhou, H. Hu, G. Shao, X. Wang, J. Qiu, Highly efficient synthesis of graphene/MnO<sub>2</sub> hybrids and their application for ultrafast oxidative decomposition of methylene blue, *Carbon* 66 (2014) 485–492.
- [116] M. Toupin, T. Brousse, D. Bélanger, Charge storage mechanism of MnO<sub>2</sub> electrode used in aqueous electrochemical capacitor, *Chem. Mater.* 16 (16) (2004) 3184–3190.
- [117] Y. Liu, M. Liu, P. Zheng, D. Ge, L. Yang, Controllable hydrogel-thermal synthesis of Mn<sub>2</sub>O<sub>3</sub>/CNT aerogels: shape evolution, growth mechanism and electrochemical properties, *Mater. Des.* 182 (2019), 108022.
- [118] A.V. Radhamani, M. Krishna Surendra, M.S. Ramachandra Rao, Tailoring the supercapacitance of Mn<sub>2</sub>O<sub>3</sub> nanofibres by nanocompositing with spinel-ZnMn<sub>2</sub>O<sub>4</sub>, *Mater. Des.* 139 (2018) 162–171.
- [119] W. Wei, X. Cui, W. Chen, D.G. Ivey, Manganese oxide-based materials as electrochemical supercapacitor electrodes, *Chem. Soc. Rev.* 40 (3) (2011) 1697–1721.
- [120] N. Yu, H. Yin, W. Zhang, Y. Liu, Z. Tang, M.-Q. Zhu, High-performance fibre-shaped all-solid-state asymmetric supercapacitors based on ultrathin MnO<sub>2</sub> nanosheet/carbon fibre cathodes for wearable electronics, *Adv. Energy Mater.* 6 (2) (2016), 1501458.
- [121] Y. Yang, S. Lee, D.E. Brown, H. Zhao, X. Li, D. Jiang, S. Hao, Y. Zhao, D. Cong, X. Zhang, Y. Ren, Fabrication of ultrafine manganese oxide-decorated carbon nanofibres for high-performance electrochemical capacitors, *Electrochim. Acta* 211 (2016) 524–532.
- [122] Y. Chen, W. Hu, H. Gan, J.-W. Wang, X.-C. Shi, Enhancing high-rate capability of MnO<sub>2</sub> film electrode deposited on carbon fibres via hydrothermal treatment, *Electrochim. Acta* 246 (Supplement C) (2017) 890–896.
- [123] S.A. Klankowski, G.P. Pandey, G. Malek, C.R. Thomas, S.L. Bernasek, J. Wu, J. Li, Higher-power supercapacitor electrodes based on mesoporous manganese oxide coating on vertically aligned carbon nanofibres, *Nanoscale* 7 (18) (2015) 8485–8494.
- [124] Y. Wen, T. Qin, Z. Wang, X. Jiang, S. Peng, J. Zhang, J. Hou, F. Huang, D. He, G. Cao, Self-supported binder-free carbon fibres/MnO<sub>2</sub> electrodes derived from disposable bamboo chopsticks for high-performance supercapacitors, *J. Alloys Compd.* 699 (2017) 126–135.
- [125] O. Pech, S. Maensiri, Electrochemical performances of electrospun carbon nanofibres, interconnected carbon nanofibres, and carbon-manganese oxide composite nanofibres, *J. Alloys Compd.* 781 (2019) 541–552.
- [126] D. Zhou, H. Lin, F. Zhang, H. Niu, L. Cui, Q. Wang, F. Qu, Freestanding MnO<sub>2</sub> nanoflakes/porous carbon nanofibres for high-performance flexible supercapacitor electrodes, *Electrochim. Acta* 161 (2015) 427–435.
- [127] K. Xu, S. Li, J. Yang, J. Hu, Hierarchical hollow MnO<sub>2</sub> nanofibres with enhanced supercapacitor performance, *J. Colloid Interface Sci.* 513 (2018) 448–454.
- [128] C.-M. Yang, B.-H. Kim, Incorporation of MnO<sub>2</sub> into boron-enriched electrospun carbon nanofibre for electrochemical supercapacitors, *J. Alloys Compd.* 780 (2019) 428–434.
- [129] H.Z. Chi, H. Zhu, L. Gao, Boron-doped MnO<sub>2</sub>/carbon fibre composite electrode for supercapacitor, *J. Alloys Compd.* 645 (Supplement C) (2015) 199–205.
- [130] D.G. Lee, B.-H. Kim, MnO<sub>2</sub> decorated on electrospun carbon nanofibre/graphene composites as supercapacitor electrode materials, *Synth. Met.* 219 (Supplement C) (2016) 115–123.
- [131] A. Śliwak, G. Gryglewicz, High-voltage asymmetric supercapacitors based on carbon and manganese oxide/oxidized carbon nanofibre composite electrodes, *Energy Technology* 2 (9–10) (2014) 819–824.
- [132] L. Wang, M. Huang, S. Chen, L. Kang, X. He, Z. Lei, F. Shi, H. Xu, Z.-H. Liu, δ-MnO<sub>2</sub> nanofibre/single-walled carbon nanotube hybrid film for all-solid-state flexible supercapacitors with high performance, *J. Mater. Chem. A* 5 (36) (2017) 19107–19115.
- [133] A.V. Radhamani, K.M. Shareef, M.S.R. Rao, ZnO/MnO<sub>2</sub> core-shell nanofibre cathodes for high performance asymmetric supercapacitors, *ACS Appl. Mater. Interfaces* 8 (44) (2016) 30531–30542.
- [134] N. Iqbal, X. Wang, A.A. Babar, G. Zainab, J. Yu, B. Ding, Flexible Fe<sub>3</sub>O<sub>4</sub>@carbon nanofibres hierarchically assembled with MnO<sub>2</sub> particles for high-performance supercapacitor electrodes, *Sci. Rep.* 7 (1) (2017), 15153.
- [135] Y. Yang, F. Yang, H. Hu, S. Lee, Y. Wang, H. Zhao, D. Zeng, B. Zhou, S. Hao, Dilute NiO/carbon nanofibre composites derived from metal organic framework fibres as electrode materials for supercapacitors, *Chem. Eng. J.* 307 (2017) 583–592.
- [136] B. Ren, M. Fan, Q. Liu, J. Wang, D. Song, X. Bai, Hollow NiO nanofibres modified by citric acid and the performances as supercapacitor electrode, *Electrochim. Acta* 92 (2013) 197–204.
- [137] S. Zhang, Y. Pang, Y. Wang, B. Dong, S. Lu, M. Li, S. Ding, NiO nanosheets anchored on honeycomb porous carbon derived from wheat husk for symmetric supercapacitor with high performance, *J. Alloys Compd.* 735 (2018) 1722–1729.
- [138] B.S. Yin, Z.B. Wang, S.W. Zhang, C. Liu, Q.Q. Ren, K. Ke, In situ growth of free-standing all metal oxide asymmetric supercapacitor, *ACS Appl. Mater. Interfaces* 8 (39) (2016) 26019–26029.
- [139] G. Cheng, W. Yang, C. Dong, T. Kou, Q. Bai, H. Wang, Z. Zhang, Ultrathin mesoporous NiO nanosheet-anchored 3D nickel foam as an advanced electrode for supercapacitors, *J. Mater. Chem. A* 3 (33) (2015) 17469–17478.
- [140] Y. Wang, S. Huang, Y. Lu, S. Cui, W. Chen, L. Mi, High-rate-capability asymmetric supercapacitor device based on lily-like Co<sub>3</sub>O<sub>4</sub> nanostructures assembled using nanowires, *RSC Adv.* 7 (7) (2017) 3752–3759.
- [141] Q. Liu, Q. Yan, S. Wu, J. Wang, H. Liu, Ultrathin porous NiO nanoflake arrays on nickel foam as binder-free electrodes for supercapacitors, *Electrochemistry* 84 (4) (2016) 219–223.
- [142] H. Wang, H. Yi, X. Chen, X. Wang, Facile synthesis of a nano-structured nickel oxide electrode with outstanding pseudocapacitive properties, *Electrochim. Acta* 105 (2013) 353–361.
- [143] G. Zhu, J. Chen, Z. Zhang, Q. Kang, X. Feng, Y. Li, Z. Huang, L. Wang, Y. Ma, NiO nanowall-assisted growth of thick carbon nanofibre layers on metal wires for fibre supercapacitors, *Chem. Commun.* 52 (13) (2016) 2721–2724.
- [144] R. Wang, D. Jin, Y. Zhang, S. Wang, J. Lang, X. Yan, L. Zhang, Engineering metal organic framework derived 3D nanostructures for high performance hybrid supercapacitors, *J. Mater. Chem. A* 5 (1) (2017) 292–302.
- [145] L. Zang, J. Zhu, Y. Xia, Facile synthesis of porous NiO nanofibres for high-performance supercapacitors, *J. Mater. Eng. Perform.* 23 (2) (2014) 679–683.
- [146] M. Kundu, L. Liu, Binder-free electrodes consisting of porous NiO nanofibres directly electrospun on nickel foam for high-rate supercapacitors, *Mater. Lett.* 144 (2015) 114–118.
- [147] Q. Li, J. Guo, D. Xu, J. Guo, X. Ou, Y. Hu, H. Qi, F. Yan, Electrospun N-doped porous carbon nanofibres incorporated with NiO nanoparticles as free-standing film electrodes for high-performance supercapacitors and CO<sub>2</sub> capture, *Small* 14 (15) (2018).
- [148] S. Alokayal, C.K. Ranaweera, Z. Wang, K. Siam, P.K. Kahol, P. Tripathi, O.N. Srivastava, B.K. Gupta, S.R. Mishra, F. Perez, X. Shen, R.K. Gupta, Nanostructured cobalt oxide and cobalt sulfide for flexible, high performance and durable supercapacitors, *Energy Storage Materials* 8 (2017) 68–76.
- [149] F. Liu, H. Su, L. Jin, H. Zhang, X. Chu, W. Yang, Facile synthesis of ultrafine cobalt oxide nanoparticles for high-performance supercapacitors, *J. Colloid Interface Sci.* 505 (2017) 796–804.
- [150] S. Ameen, M.S. Akhtar, H.K. Seo, Y.S. Kim, H.S. Shin, Influence of Sn doping on ZnO nanostructures from nanoparticles to spindle shape and their photoelectrochemical properties for dye sensitized solar cells, *Chem. Eng. J.* 187 (2012) 351–356.
- [151] N. Iqbal, X. Wang, J. Ge, J. Yu, H.-Y. Kim, S.S. Al-Deyab, M. El-Newehy, B. Ding, Cobalt oxide nanoparticles embedded in flexible carbon nanofibres: attractive material for supercapacitor electrodes and CO<sub>2</sub> adsorption, *RSC Adv.* 6 (57) (2016) 52171–52179.
- [152] S.H. Kim, Y.I. Kim, J.H. Park, J.M. Ko, Cobalt-manganese oxide/carbon-nanofibre composite electrodes for supercapacitors, *Int. J. Electrochem. Sci.* 4 (11) (2009) 1489–1496.
- [153] J. Bhagwan, V. Sivasankaran, K.L. Yadav, Y. Sharma, Porous, one-dimensional and high aspect ratio nanofibre network of cobalt manganese oxide as a high performance material for aqueous and solid-state supercapacitor (2 V), *J. Power Sources* 327 (2016) 29–37.
- [154] J. Xu, F. Zheng, C. Xi, Y. Yu, L. Chen, W. Yang, P. Hu, Q. Zhen, S. Bashir, Facile preparation of hierarchical vanadium pentoxide (V<sub>2</sub>O<sub>5</sub>)/titanium dioxide (TiO<sub>2</sub>) heterojunction composite nano-arrays for high performance supercapacitor, *J. Power Sources* 404 (2018) 47–55.
- [155] N.M. Ndiaye, B.D. Ngom, N.F. Sylla, T.M. Masikhwa, M.J. Madito, D. Momodu, T. Ntsoane, N. Manyala, Three dimensional vanadium pentoxide/graphene foam composite as positive electrode for high performance asymmetric electrochemical supercapacitor, *J. Colloid Interface Sci.* 532 (2018) 395–406.
- [156] R. Thangappan, S. Kalaiselvam, A. Elayaperumal, R. Jayavel, Synthesis of graphene oxide/vanadium pentoxide composite nanofibres by electrospinning for supercapacitor applications, *Solid State Ionics* 268 (Part B) (2014) 321–325.
- [157] B.-H. Kim, C.H. Kim, K.S. Yang, A. Rahy, D.J. Yang, Electrospun vanadium pentoxide/carbon nanofibre composites for supercapacitor electrodes, *Electrochim. Acta* 83 (2012) 335–340.
- [158] G. Huang, C. Li, J. Bai, X. Sun, H. Liang, Controllable-multichannel carbon nanofibres-based amorphous vanadium as binder-free and conductive-free electrode materials for supercapacitor, *Int. J. Hydrog. Energy* 41 (47) (2016) 22144–22154.
- [159] T. Prasankumar, V.S. Irthaza Aazem, P. Raghavan, K. Prem Ananth, S. Biradar, R. Ilangoan, S. Jose, Microwave assisted synthesis of 3D network of Mn/Zn bimetallic oxide-high performance electrodes for supercapacitors, *J. Alloys Compd.* 695 (2017) 2835–2843.

- [160] H. Mu, J. Bai, C. Li, W. Sun, Strong physisorption and superb thermal stability of carbon nanofibres carried  $\text{Cu}_2\text{O-V}_2\text{O}_5$  enabling the flexible and long-cycling supercapacitor, *J. Alloys Compd.* 775 (2019) 872–882.
- [161] D.D. Potphode, S.P. Mishra, P. Sivaraman, M. Patri, Asymmetric supercapacitor devices based on dendritic conducting polymer and activated carbon, *Electrochim. Acta* 230 (2017) 29–38.
- [162] G.A. Snook, P. Kao, A.S. Best, Conducting-polymer-based supercapacitor devices and electrodes, *J. Power Sources* 196 (1) (2011) 1–12.
- [163] D. Aradilla, S. Sadki, G. Bidan, Beyond conventional supercapacitors: hierarchically conducting polymer-coated 3D nanostructures for integrated on-chip micro-supercapacitors employing ionic liquid electrolytes, *Synth. Met.* 247 (2019) 131–143.
- [164] P. Asen, S. Shahrokhian, A.I. zad, Ternary nanostructures of  $\text{Cr}_2\text{O}_3/\text{graphene oxide}/\text{conducting polymers}$  for supercapacitor application, *J. Electroanal. Chem.* 823 (2018) 505–516.
- [165] Y.G. Wang, H.Q. Li, Y.Y. Xia, Ordered whiskerlike polyaniline grown on the surface of mesoporous carbon and its electrochemical capacitance performance, *Adv. Mater.* 18 (19) (2006) 2619–2623.
- [166] L. Xia, H. Huang, Z. Fan, D. Hu, D. Zhang, A.S. Khan, M. Usman, L. Pan, Hierarchical macro-/meso-/microporous oxygen-doped carbon derived from sodium alginate: a cost-effective biomass material for binder-free supercapacitors, *Mater. Des.* 182 (2019), 108048.
- [167] S. Sankar, A.T.A. Ahmed, A.I. Inamdar, H. Im, Y.B. Im, Y. Lee, D.Y. Kim, S. Lee, Biomass-derived ultrathin mesoporous graphitic carbon nanoflakes as stable electrode material for high-performance supercapacitors, *Mater. Des.* 169 (2019), 107688.
- [168] K. Zhang, L.L. Zhang, X.S. Zhao, J. Wu, Graphene/polyaniline nanofibre composites as supercapacitor electrodes, *Chem. Mater.* 22 (4) (2010) 1392–1401.
- [169] P. Haldar, S. Biswas, V. Sharma, A. Chowdhury, A. Chandra,  $\text{Mn}_3\text{O}_4$ -polyaniline-graphene as distinctive composite for use in high-performance supercapacitors, *Appl. Surf. Sci.* 491 (2019) 171–179.
- [170] Z. Huang, L. Li, Y. Wang, C. Zhang, T. Liu, Polyaniline/graphene nanocomposites towards high-performance supercapacitors: a review, *Composites Communications* 8 (2018) 83–91.
- [171] K. Li, X. Liu, S. Chen, W. Pan, J. Zhang, A flexible solid-state supercapacitor based on graphene/polyaniline paper electrodes, *Journal of Energy Chemistry* 32 (2019) 166–173.
- [172] N. Song, Y. Wu, W. Wang, D. Xiao, H. Tan, Y. Zhao, Layer-by-layer in situ growth flexible polyaniline/graphene paper wrapped by  $\text{MnO}_2$  nanoflowers for all-solid-state supercapacitor, *Mater. Res. Bull.* 111 (2019) 267–276.
- [173] J. Ji, R. Li, H. Li, Y. Shu, Y. Li, S. Qiu, C. He, Y. Yang, Phytic acid assisted fabrication of graphene/polyaniline composite hydrogels for high-capacitance supercapacitors, *Compos. Part B* 155 (2018) 132–137.
- [174] Q. Zhou, T. Wei, J. Yue, L. Sheng, Z. Fan, Polyaniline nanofibres confined into graphene oxide architecture for high-performance supercapacitors, *Electrochim. Acta* 291 (2018) 234–241.
- [175] A. Ladrón-de-Guevara, A. Boscá, J. Pedrós, E. Climent-Pascual, A. de Andrés, F. Calle, J. Martínez, Reduced graphene oxide/polyaniline electrochemical supercapacitors fabricated by laser, *Appl. Surf. Sci.* 467–468 (2019) 691–697.
- [176] M. Barakzei, M. Montazer, F. Sharif, T. Norby, A. Chatzitakis, A textile-based wearable supercapacitor using reduced graphene oxide/polypyrrole composite, *Electrochim. Acta* 305 (2019) 187–196.
- [177] S. Li, Y. Chang, G. Han, H. Song, Y. Chang, Y. Xiao, Asymmetric supercapacitor based on reduced graphene oxide/ $\text{MnO}_2$  and polypyrrole deposited on carbon foam derived from melamine sponge, *J. Phys. Chem. Solids* 130 (2019) 100–110.
- [178] Y. Han, Z. Zhang, M. Yang, T. Li, Y. Wang, A. Cao, Z. Chen, Facile preparation of reduced graphene oxide/polypyrrole nanocomposites with urchin-like microstructure for wide-potential-window supercapacitors, *Electrochim. Acta* 289 (2018) 238–247.
- [179] D. Sarmah, A. Kumar, Ion beam modified molybdenum disulfide-reduced graphene oxide/polypyrrole nanotubes ternary nanocomposite for hybrid supercapacitor electrode, *Electrochim. Acta* 312 (2019) 392–410.
- [180] X. Guo, N. Bai, Y. Tian, L. Gai, Free-standing reduced graphene oxide/polypyrrole films with enhanced electrochemical performance for flexible supercapacitors, *J. Power Sources* 408 (2018) 51–57.
- [181] F. Su, M. Miao, Flexible, high performance two-ply yarn supercapacitors based on irradiated carbon nanotube yarn and PEDOT/PSS, *Electrochim. Acta* 127 (2014) 433–438.
- [182] Q. Yang, S.-K. Pang, K.-C. Yung, Study of PEDOT-PSS in carbon nanotube/conducting polymer composites as supercapacitor electrodes in aqueous solution, *J. Electroanal. Chem.* 728 (2014) 140–147.
- [183] L. Gao, X. Mao, H. Zhu, W. Xiao, F. Gan, D. Wang, Electropolymerization of PEDOT on CNTs conductive network assembled at water/oil interface, *Electrochim. Acta* 136 (2014) 97–104.
- [184] B. Gupta, M. Mehta, A. Melvin, R. Kamalakannan, S. Dash, M. Kamruddin, A.K. Tyagi, Poly (3,4-ethylenedioxythiophene) (PEDOT) and poly (3,4-ethylenedioxythiophene)-few walled carbon nanotube (PEDOT-FWCNT) nanocomposite based thin films for Schottky diode application, *Mater. Chem. Phys.* 147 (3) (2014) 867–877.
- [185] J. Jang, J. Bae, M. Choi, S.-H. Yoon, Fabrication and characterization of polyaniline coated carbon nanofibre for supercapacitor, *Carbon* 43 (13) (2005) 2730–2736.
- [186] K.S. Ryu, K.M. Kim, N.G. Park, Y.J. Park, S.H. Chang, Symmetric redox supercapacitor with conducting polyaniline electrodes, *J. Power Sources* 103 (2) (2002) 305–309.
- [187] K.S. Ryu, K.M. Kim, Y.J. Park, N.G. Park, M.G. Kang, S.H. Chang, Redox supercapacitor using polyaniline doped with Li salt as electrode, *Solid State Ionics* 152–153 (2002) 861–866.
- [188] F. Faverolle, A.J. Attias, B. Bloch, P. Audebert, C.P. Andrieux, Highly conducting and strongly adhering polypyrrole coating layers deposited on glass substrates by a chemical process, *Chem. Mater.* 10 (3) (1998) 740–752.
- [189] K. Lota, V. Khomenko, E. Frackowiak, Capacitance properties of poly(3,4-ethylenedioxythiophene)/carbon nanotubes composites, *J. Phys. Chem. Solids* 65 (2–3) (2004) 295–301.
- [190] X. Cao, H.-Y. Zeng, S. Xu, J. Yuan, J. Han, G.-F. Xiao, Facile fabrication of the polyaniline/layered double hydroxide nanosheet composite for supercapacitors, *Appl. Clay Sci.* 168 (2019) 175–183.
- [191] M. Padmini, P. Elumalai, P. Thomas, Symmetric supercapacitor performances of  $\text{CaCu}_3\text{Ti}_4\text{O}_{12}$  decorated polyaniline nanocomposite, *Electrochim. Acta* 292 (2018) 558–567.
- [192] B. Sari, M. Talu, F. Yildirim, Electrochemical polymerization of aniline at low supporting-electrolyte concentrations and characterization of obtained films, *Russ. J. Electrochem.* 38 (7) (2002) 707–713.
- [193] F. Ke, J. Tang, S. Guang, H. Xu, Controlling the morphology and property of carbon fibre/polyaniline composites for supercapacitor electrode materials by surface functionalization, *RSC Adv.* 6 (18) (2016) 14712–14719.
- [194] H. Mi, X. Zhang, S. An, X. Ye, S. Yang, Microwave-assisted synthesis and electrochemical capacitance of polyaniline/multi-wall carbon nanotubes composite, *Electrochem. Commun.* 9 (12) (2007) 2859–2862.
- [195] Q. Wu, Y. Xu, Z. Yao, A. Liu, G. Shi, Supercapacitors based on flexible graphene/polyaniline nanofibre composite films, *ACS Nano* 4 (4) (2010) 1963–1970.
- [196] J. Zhang, J. Jiang, H. Li, X.S. Zhao, A high-performance asymmetric supercapacitor fabricated with graphene-based electrodes, *Energy Environ. Sci.* 4 (10) (2011) 4009–4015.
- [197] K. Jin, W. Zhang, Y. Wang, X. Guo, Z. Chen, L. Li, Y. Zhang, Z. Wang, J. Chen, L. Sun, T. Zhang, In-situ hybridization of polyaniline nanofibres on functionalized reduced graphene oxide films for high-performance supercapacitor, *Electrochim. Acta* 285 (2018) 221–229.
- [198] D. Yang, W. Ni, J. Cheng, Z. Wang, C. Li, Y. Zhang, B. Wang, Omnidirectional porous fibre scrolls of polyaniline nanopillars array-N-doped carbon nanofibres for fibre-shaped supercapacitors, *Materials Today Energy* 5 (2017) 196–204.
- [199] H. Luo, H. Lu, J. Qiu, Carbon fibres surface-grown with helical carbon nanotubes and polyaniline for high-performance electrode materials and flexible supercapacitors, *J. Electroanal. Chem.* 828 (2018) 24–32.
- [200] C.J. Raj, B.C. Kim, W.J. Cho, W.G. Lee, S.D. Jung, Y.H. Kim, S.Y. Park, K.H. Yu, Highly flexible and planar supercapacitors using graphite flakes/polypyrrole in polymer lapping film, *ACS Appl. Mater. Interfaces* 7 (24) (2015) 13405–13414.
- [201] W. Sun, R. Zheng, X. Chen, Symmetric redox supercapacitor based on micro-fabrication with three-dimensional polypyrrole electrodes, *J. Power Sources* 195 (20) (2010) 7120–7125.
- [202] S. Huang, Y. Han, S. Lyu, W. Lin, P. Chen, S. Fang, A facile one-step approach for the fabrication of polypyrrole nanowire/carbon fibre hybrid electrodes for flexible high performance solid-state supercapacitors, *Nanotechnology* 28 (43) (2017).
- [203] F.M. Guo, R.Q. Xu, X. Cui, L. Zhang, K.L. Wang, Y.W. Yao, J.Q. Wei, High performance of stretchable carbon nanotube-polypyrrole fibre supercapacitors under dynamic deformation and temperature variation, *J. Mater. Chem. A* 4 (23) (2016) 9311–9318.
- [204] Y. Chang, G. Han, Y. Xiao, Y. Chang, H. Song, M. Li, Y. Li, Y. Zhang, Internal tandem flexible and compressible electrochemical capacitor based on polypyrrole/carbon fibres, *Electrochim. Acta* 257 (2017) 335–344.
- [205] A.A.B. Hamra, H.N. Lim, S.M. Hafiz, S. Kamaruzaman, S.A. Rashid, R. Yunus, M. Altarawneh, Z.T. Jiang, N.M. Huang, Performance stability of solid-state polypyrrole-reduced graphene oxide-modified carbon bundle fibre for supercapacitor application, *Electrochim. Acta* 285 (2018) 9–15.
- [206] K. Zhang, J. Xu, X. Zhu, L. Lu, X. Duan, D. Hu, L. Dong, H. Sun, Y. Gao, Y. Wu, Poly(3,4-ethylenedioxythiophene) nanorods grown on graphene oxide sheets as electrochemical sensing platform for rutin, *J. Electroanal. Chem.* 739 (1) (2015) 66–72.
- [207] G.P. Pandey, A.C. Rastogi, Solid-state supercapacitors based on pulse polymerized poly(3,4-ethylenedioxythiophene) electrodes and ionic liquid gel polymer electrolyte, *J. Electrochem. Soc.* 159 (10) (2012) A1664–A1671.
- [208] M. Rajesh, C.J. Raj, R. Manikandan, B.C. Kim, S.Y. Park, K.H. Yu, A high performance PEDOT/PEDOT symmetric supercapacitor by facile in-situ hydrothermal polymerization of PEDOT nanostructures on flexible carbon fibre cloth electrodes, *Materials Today Energy* 6 (2017) 96–104.
- [209] J. Garcia-Torres, C. Crean, Ternary composite solid-state flexible supercapacitor based on nanocarbons/manganese dioxide/PEDOT:PSS fibres, *Mater. Des.* 155 (2018) 194–202.
- [210] X. Gong, S. Li, P.S. Lee, A fibre asymmetric supercapacitor based on  $\text{FeOOH}/\text{PPy}$  on carbon fibres as an anode electrode with high volumetric energy density for wearable applications, *Nanoscale* 9 (30) (2017) 10794–10801.